バイオサイエンス研究科　博士論文要旨

所　属 (主指導教官)	バイオサイエンス研究科　動物細胞工学　(河野　憲二　教授)		
氏　名	佐野　裕美	提　出	平成 15 年 10 月 7 日
題　目	Dual control of the basal ganglia neural circuitry through the striatopallidal medium spiny neurons (線条体－淡蒼球中等大有棘ニューロンを介する大脳基底核神経回路の二重制御)		

要旨

The basal ganglia mediate a wide variety of psychomotor functions, including motor control, motor planning, and behavioral learning. The nigrostriatal dopamine (DA)-producing neurons play a critical role in the basal ganglia functions. Striatal projection neurons are composed of two subpopulations of γ-aminobutyric acid (GABA)-producing medium spiny neurons that constitute the so-called direct and indirect pathways. The striatonigral medium spiny neurons in the direct pathway provide monosynaptic inhibition to the output nuclei, whereas the striatopallidal medium spiny neurons in the indirect pathway inhibit the globus pallidum (GP). The GP neurons send inhibitory efferents to the output nuclei or the subthalamic nucleus (STN), and the STN provides an alternative route to the output nuclei. DA acts to regulate oppositely the activity of the striatonigral medium spiny neurons and striatopallidal medium spiny neurons, and the actions appear to be mediated by the differential expression of DA receptor subtypes. Striatal aspiny interneurons producing acetylcholine (ACh) or GABA also express different subtypes of DA receptors. The neural mechanism by which DA controls the basal ganglia circuitry through various populations of striatal neurons is not yet fully understood.

Immunotoxin-mediated cell targeting (IMCT) is a technique for conditional cell ablation in transgenic animals. IMCT has been utilized to eliminate specific neuronal types from a complex neural circuitry. In the strategy of IMCT, transgenic mice are generated that express human interleukin-2 receptor α-subunit (IL-2Rα) under the control of a cell type-specific promoter, and these mice are then treated with a recombinant immunotoxin (IT). In the present study, IMCT was applied to ablate the neuronal types expressing dopamine D2 receptor (D2R) in the dorsal striatum. To express IL-2Rα under the control of the D2R gene, the IL-2Rα gene

cassette was introduced into the mouse D2R locus with gene targeting. The expression pattern of IL-2Rα in mice heterozygous for the mutation was detected in some brain regions where endogenous D2R expression was detected. Injection of IT into the striatum induced a selective ablation of the striatopallidal medium spiny neurons and the cholinergic interneurons in the mutants. However, IT injection did not affect the anatomy of nigrostriatal DA neurons and the metabolism of DA in the mutants. In addition, the injection reduced the ligand binding sites in the striatum for D2 class receptors but not for D1 class receptors.

The ablation of the striatal D2R-expressing neurons caused abnormalities in motor behavior, which were characterized by a hyperactivity of spontaneous movement and an attenuation of DA-induced hyperactivity. The ablation of these neurons caused upregulation of glutamic acid decarboxylase (GAD67) mRNA in the GP and downregulation of cytochrome oxidase activity in the STN, whereas it did not affect the expression of substance P mRNA in the striatonigral medium spiny neurons. The ablation reduced DA-induced expression of the immediate early genes (IEGs) in the striatonigral medium spiny neurons but not in the GP and STN. In addition, the mice treated with a selective cholinergic neurotoxin showed no apparent change in spontaneous motor behavior and they exhibited a modest increase in DA-induced behavior. The lesion of cholinergic interneurons increased DA-induced IEGs expression in the striatonigral medium spiny neurons.

The results obtained from the behavioral study suggest that ablation of the striatopallidal medium spiny neurons are predominantly responsible for the increased spontaneous locomotion and the impaired DA-induced motor activation in the mutants. The results obtained from the study of gene expression in the basal ganglia circuitry suggest that the striatopallidal medium spiny neurons normally suppress spontaneous movement through inhibition of the GP neurons. But these neurons increase motor activity in response to DA stimulation through not only disinhibition of the GP neurons but also facilitation of the striatonigral medium spiny neurons.

Dual control of the basal ganglia neural circuitry through the striatopallidal medium spiny neurons

奈良先端科学技術大学院大学
バイオサイエンス研究科　動物細胞工学部門
（河野　憲二　教授）

平成 15 年 10 月 7 日提出

Contents

Introduction

The basal ganglia mediate a wide variety of psychomotor functions, including motor control, motor planning, and behavioral learning (Graybiel, 1995; Kimura, 1995; Schultz et al., 1997). A number of behavioral and physiological evidence indicate that the nigrostriatal dopaminergic pathway plays a central role in the basal ganglia functions (Wickens, 1990; Graybiel et al., 1994). The importance of dopamine (DA) in the basal ganglia is also exhibited by the symptoms of Parkinson' disease, which is caused by selective loss of a group of DA neurons in the ventral midbrain (Rinne, 1993; Young, 1999). Recent studies with mutant mice deficient in DA biosynthesis provide genetic evidence for an essential role of DA in motor control, emotional learning, and feeding behavior during postnatal development (Zhou et al., 1995; Nishii et al., 1998; Szczypka et al., 1999a, b; Szczypka et al., 2001).

The dorsal striatum, the most prominent portion of the basal ganglia, receives excitatory inputs from many areas of the cerebral cortex and projects to the output nuclei of the basal ganglia, the substantia nigra pars reticulata (SNr) and entopeduncular nucleus (EPN) (Alexander and Crucher, 1990; DeLong, 1990; Parent and Hazrati, 1995; Gerfen and Wilson, 1996). Striatal projection neurons are composed of two subpopulations of γ-aminobutyric acid (GABA)-producing medium spiny neurons that constitute the so-called direct and indirect pathways. The striatonigral medium spiny neurons in the direct pathway contain substance P (SP) and provide monosynaptic inhibition to the output nuclei, whereas the striatopallidal medium spiny neurons in the indirect pathway contain enkephalin (ENK) and inhibit the globus pallidum (GP). The GP neurons send inhibitory efferents to the output nuclei or the subthalamic nucleus (STN), and the STN provides an alternative route to the output nuclei (Gerfen, 1992a, b). The standard model of the neural circuitry suggests that basal ganglia

functions are dependent on the balance between opposing inputs from the direct and indirect pathways, although the model is challenged by recent data, such as the presence of direct corticosubthalamic pathway (Nambu et al., 2002) and the rhythmic pattern of neuronal firing after DA depletion (Bergman et al., 1998; Bevan et al., 2002).

DA acts to regulate oppositely the activity of the striatonigral medium spiny neurons and the striatopallidal medium spiny neurons (Nicola et al., 2000), and the actions appear to be mediated by different DA receptor subtypes. DA receptors are classified into two classes, the D1 class (D1R and D5R) and the D2 class (D2R, D3R, and D4R), based upon pharmacological and biochemical criteria (Civelli et al., 1993; Gingrich and Caron, 1993). Neuropharmacological and neurophysiological data point to a facilitating effect of D1R on the striatonigral medium spiny neurons and suppressing effect of D2R on the striatopallidal medium spiny neurons (Weick and Walters, 1987; Walters et al., 1987; Gerfen et al., 1995). D1R and D2R appear to be localized in the striatonigral and striatopallidal medium spiny neurons, respectively, although colocalization of these two subtypes in some neurons has been suggested (Lester et al., 1993; Surmeier et al., 1996; Aizman et al., 2001). Striatal aspiny interneurons producing acetylcholine (ACh) or GABA also express different subtypes of the D1 class or D2 class receptors (Kawaguchi et al., 1995). The neural mechanism by which DA controls the basal ganglia circuitry through various populations of striatal neurons is not yet fully understood.

In the past few years a number of laboratories has turned to gene targeting as a more precise to determining distinct functions of DA receptor subtypes. For example, studies on D1 and D2 knock-out mice revealed significant differences with regard motor and motivated behavior influenced by these receptors. Whereas D1 knock-out mice exhibited locomotor

hyperactivity and fail to mediate the locomotor stimulant effects of cocaine and amphetamine (Xu et al., 1994a, b). D2 knock-out mice showed locomotor hypoactivity and postural abnormalities, and they fail to experience the rewarding effects of opioid drugs (Baik et al., 1995; Maldonado et al., 1997). Moreover, studies on D1 and D2 receptor knock-out mice have provided direct evidence for D1 and D2 receptor-mediated control of expression of the striatal peptides dynorphin and enkephalin, respectively (Drago et al., 1994; Xu et al., 1994a; Baik et al., 1995). However the neural mechanisms by which DA controls the motor and motivated behavior are not fully revealed.

Immunotoxin-mediated cell targeting (IMCT) is a technique for conditional cell ablation in transgenic animals (Kobayashi et al., 1995a; Kobayashi et al., 1996). In the strategy of IMCT (Kobayashi et al., 1995a), transgenic mice are generated that express human interleukin-2 receptor α-subunit (IL-2Rα) under the control of a cell type-specific promoter. These mice are then treated with a recombinant immunotoxin (IT), which consists of the variable regions of the anti-IL-2Rα monoclonal antibody fused to a bacterial exotoxin, resulting in ablation of target cell types. IMCT has been utilized to eliminate specific neuronal types from a complex neural circuitry (Sawada et al., 1998; Watanabe et al., 1998; Kaneko et al., 2000; Yoshida et al., 2001; Hikida et al., 2001; Hikida et al., 2003; Kitabatake et al., 2003). In the present study, the neuronal types expressing D2R subtypes in the dorsal striatum are ablated by IMCT. A selective localization of D2R is shown in the majority of the striatopallidal medium spiny neurons and cholinergic interneurons. The behavioral influences of neuronal elimination on basal ganglia function that depends on DA transmission are examined and the neural circuitry involved in the behavior are analyzed. In addition, the influences of chemical lesion of cholinergic interneurons on basal ganglia function are

examined. These results indicate that the striatopallidal medium spiny neurons play an essential role in dual control of motor behavior that includes the suppression of spontaneous behavior and the full expression of DA-induced behavior. These findings propose a model in which the striatopallidal medium spiny neurons coordinate the basal ganglia circuitry depending on the state of DA transmission.

Materials and Methods

Generation of mutant mice

Phage clones containing the mouse D2R gene were isolated from a 129SV/J genomic DNA library using λFIX™II vector (Stratagene). The targeting vector, containing the 5' -homologous region of 2.4 kb, the IL-2Rα gene cassette having the polyadenylation signals derived from pDIL vector (Kobayashi et al., 1995a), the phosphoglycerate kinase-1-*neo* gene cassette, and the 3'-homologous region of 7.6 kb, and the diphtheria toxin A-fragment gene cassette was introduced into the 5'-end of the targeting vector (see Figure 1A). Gene targeting with ES cells was performed essentially as described by Kobayashi et al. (1995b). E14 ES cells were cultured on feeder layers prepared from neomycin-resistant primary fibroblast cells in Dulbecco's modified Eagle's medium (GIBCO) supplemented with 20% of fetal bovine serum (Laboratories Inc., HyClone, Lot No. AFA4819), 1000 units/ml leukemia inhibitory factor (Chemicon), penicillin-streptomycin (GIBCO), 1 X non-essential amino acids (GIBCO), and 0.1 mM β -mercaptoethanol (Sigma) at 37℃ in a 5 % CO_2 incubator. ES cells (5 X 10^7 cells) were electroporated (240 V, 500 μF) by GENE PULSUR (Bio Rad) with the linearized targeting vector (10 μg) and were selected in medium containing 0.25 mg/ml G418 (GIBCO) for 10 days. Individually picked colonies were analyzed by Southern blotting with a *Hind*III-*Eco*RI fragment (Probe A), *Eco*RI-*Eco*RI fragment (Probe B) and *BamH*I–*Sph*I fragment (Probe C) labeled with ^{32}P. Correctly targeted ES clones were microinjected into C57BL6/J blastocysts, which were implanted into the uterine horns of pseudopregnant mothers, to produce chimeric mice. Male chimeric mice were crossed with C57BL6/J female mice, and germ line transmission was judged by the coat color of the offsprings. Mice heterozygous for the D2R mutation were identified by Southern blotting of tail DNA.

Heterozygous mice were mated with C57BL6/J mice for more than seven generations. Animal care and handling procedures were in accordance with the guidelines established by the Animal Center of Nara Institute of Science and Technology and the Experimental Animal Center of Fukushima Medical University.

Genomic typing

Southern blotting was used to identify the correctly targeted ES clones and the genotypes of the mice. ES cells or tails were incubated for over night at 55℃ in lysis buffer [100 mM NaCl, 500 mM Tris-HCl (pH 8.0), 10 mM EDTA and 1% SDS] and Proteinase K (150 ng/ml, Roche). After incubation, genomic DNA was extracted and digested by *BamH*I or *Apa*I for over night. Then, digested genomic DNA samples loaded onto a 0.8% agarose gel and ran at 40 V for 5 hr. The gel was photographed and the DNA was blotted onto a nylon membrane (Hybond-XL, Amersham Pharmacia Biotech). The probes were labeled using Megaprime DNA Labelling System (Amersham Pharmacia Biotech) and [α–^{32}P] dCTP (Amersham Pharmacia Biotech). The membranes were hybridized with the ^{32}P-labelled Probe A, Probe B or Probe C in hybridization buffer [50% formamide, 5 X SSPE, 5 X Denhardt's, 0.3% SDS and 0.1 mg/ml salmon sperm DNA] overnight at 42℃ and rinsed twice in 2 X SSC and 10% SDS. The membranes were exposed to BAS-MS2040 imaging plates (Fuji film).

Stereotaxic surgery

Mice were deeply anesthetized with sodium pentobarbital (Dainippon Pharmaceutical Co., LTD, 50 mg/kg, *i.p.*), and subjected to unilateral or bilateral intrastriatal injection of 10 μg/ml IT (anti-Tac(Fv)-PE38) (Kreitman et al., 1994) solution. IT was diluted with 0.01 M

phosphate buffered saline (PBS) containing 0.5 mg/ml mouse serum albumin (Sigma). The IT solution or PBS (0.5 μl/site) was injected into six sites in one side of the striatum through a glass micropipette (diameter in 50 μm), which was stereotaxically introduced by using the coordinates according to an atlas of the mouse brain (Paxinos and Flanklin, 2001). The anteroposterior, mediolateral and dorsoventral coordinates from bregma or dura were 1.20/1.25/2.00 mm (site 1), 1.20/2.00/2.00 mm (site 2), 0.50/1.50/2.00 mm (site 3), 0.50/2.25/2.50 mm (site 4), -0.20/2.50/2.50 mm (site 5), and -0.70/2.75/2.50 mm (site 6) (see Figure 2B). Injection was carried out at a constant flow rate of 0.25 μl/min with microinfusion pump (ESP-32, EICOM) connected to the glass micropipette.

For intrastriatal administration of acetylethylcholine mustard aziridinium ion (acetyl AF64A, Sigma), 2 mM AF64A solution was prepared as described (Fisher et al., 1982) with minor modifications. Acetyl AF64A was rapidly dissolved in saline. The pH was adjusted to between 11.5 and 11.7 with 1 M NaOH and maintained at pH 11.5 for 30 min. The pH was adjusted then to pH 6.0 to 7.0 using 1 N HCl before final titration to pH 7.4 with solid $NaHCO_3$. Saline was added to bring the final concentration of AF64A to 2 mM. AF64A solution or saline (1 μl/site) was injected through a glass micropipette (diameter in 50 μm) by using the coordinates (mm) anterior 1.00, lateral 1.50, and ventral 2.00 from bregma and dura. Administration was carried out at a constant flow rate of 0.25 μl/min with a microinfusion pump (ESP-32, EICOM).

After the experiments, the placement sites of a glass micropipette within the striatum were confirmed by histological examination with Nissl staining.

Histology

(1) Nissl staining

Nissl staining was performed as described (Roberts et al., 1993) with minor modifications. Mice were deeply anesthetized with sodium pentobarbital and perfused transcardially with 4% paraformaldehyde (Wako) in 0.1 M phosphate buffer or PB (pH 7.4). After cryoprotection with 30% (w/v) sucrose in 0.1M PB, the brains were cut into frontal sections on a freezing microtome (CM1900, Leica). Sections (30 μm thick) were mounted on silanized slides (S3003, DAKO), dehydrated through graded ethanol solutions (70%, 80%, 90%, 95%, 100%; 5 min each), rehydrated through graded ethanol solutions (100%, 95%, 90%, 80%, 70%; 5 min each) and placed into water. Then, sections were immersed in 5% cresyl violet solution (Chroma-Gesellschaft) for 10 min, differentiated in a graded ethanol solutions (70%, 80%, 90%, 100%; 5 min each) and coverslipped after 5 min in xylene.

(2) In situ hybridization

In situ hybridization was performed as described (Kaneda et al., 1991) with some modifications. Mice were deeply anesthetized with sodium pentobarbital. The brains were quickly removed and cut into frontal sections on a freezing microtome (CM1900, Leica). Fresh-frozen sections (10 μm thick) were mounted on APS-coated slide glass (Matsunami) and fixed in a solution of 4% paraformaldehyde in 0.1 M PB and treated with 0.1 M triethanolamine (pH 8.0) containing 0.25% acetic anhydride. The sections were hybridized at 58℃ with riboprobes labeling by in vitro transcription with [^{35}S] CTPαS (Perkin Elmer, 1 X 10^8 cpm/ml) or digoxigenin-11-UTP (Roche, 1 mg/ml) in hybridization buffer [50% formamide, 2 X SSC, 10 mM Tris-HCl (pH 8.0), 10 μg/ml salmon sperm DNA, 1 X Denhardt's, 10% dextran sulfate and 0.2% SDS] . Subsequently, following washes in 2 X SSC

at 60℃ and 0.2 X SSC at 60℃, the sections were treated with 2 μg/ml RNase A at 37℃ for 1 hr, washed twice with 2 X SSC at room temperature and transferred to 0.2 X SSC. Sections hybridized with radiolabeled cRNA probes were dehydrated in graded ethanol solutions (70%, 80%, 90%, 100%, 100%; 5 min each) and exposed to BAS-MS2040 imaging plates (Fuji film). Sections hybridized with digoxigenin-labeled cRNA probes were incubated for 2 hr with alkaline phosphatase-conjugated anti-digoxigenin antiserum (1:1000, Roche) and then with 0.45 mg/ml nitroblue tetrazilium (Roche) / 0.18 mg/ml bromo-choloro-indolylphosphate (Roche).

Antisense riboprobes used were complementary to a part of mouse D1R mRNA, mouse D2R mRNA, human IL-2Rα mRNA, mouse SP mRNA, and mouse GAD67 mRNA. There was no significant hybridization signal in control experiments using the corresponding sense probes.

(3) Immunohistochemistry

Immunohistochemistry was carried out with the avidin-biotin-complex method as described (Lee et al., 1997) with minor modifications. Mice were deeply anesthetized with sodium pentobarbital and perfused transcardially with 4% paraformaldehyde in 0.1 M PB or 0.2% formaldehyde and 75% saturated picric acid (Wako) in 0.1 M PB. The brains were quickly removed and placed for over night at 4℃ in 4% paraformaldehyde or 2% formaldehyde and 75% saturated picric acid in 0.1 M PB. After cryoprotection with 30% (w/v) sucrose in 0.1 M PB, the brains were cut into frontal sections on a freezing microtome (CM1900, Leica). Free floating sections (30 μm thick) were incubated in 1% hydrogen peroxide for 30 min at room temperature, 5% normal swine serum (DAKO) for 1 hr at room temperature, and for 2 days at 4℃ with primary antibodies against synthetic C-terminal nonadecapeptide of

preproenkephalin (1 μg/ml, Lee et al., 1997), synthetic C-terminal pentadecapeptide of preprotachykinin A (1 μg/ml, Lee et al., 1997), choline acetyltransferase (1:3000, Ichikawa et al., 1997), parvalbumin (1:1000, Sigma), somatostatin (1:100, Medac), calretinin (1:1000, Chemicon), tyrosine hydroxylase (10 μg/ml, Roche), dopamine transporter (1:5000, Chemicon), c-*fos* (1:5000, Santa Cruz Biotechnology) and *zif268* (1:1000, Santa Cruz Biotechnology). Sections were then washed in 0.01M PBS for three times and incubated in biotinylated anti-guinea pig IgG (1:1000, Chemicon), rabbit IgG (1:1000, Jackson ImmunoResearch Laboratories), mouse IgG (1:1000, Jackson ImmunoResearch Laboratories), or rat IgG antibody (1:1000, Cappel Pharmaceuticals) for 2 hr at room temperature. The incubations were carried out in 0.01M PBS following by a rinse with 0.01M PBS for two times. The sections were further incubated for 2 hr with avidin-biotinylatd peroxidase complex (Vectastain Elite ABC kit, Vector Laboratories) in 0.01 M PBS. Then, the bound peroxidase was developed by reaction with 0.2 mg/ml 3,3'-diaminobenzidine-4HCl (Dojindo) and 0.001% H_2O_2 in 50 mM Tris-HCl (pH 7.6). For *c-fos* and *zif268* immunostaining, mice were administered with methamphetamine (METH, 6 mg/kg, *i.p.*) 1.5 hr before perfusion.

(4) CO histochemistry

CO histochemistry was done as described (Vila et al. 1996). Mice were anesthetized with sodium pentobarbital and perfused transcardially with 4% paraformaldehyde in 0.1 M PB. The brains were quickly removed and placed for over night at 4℃ in 4% paraformaldehyde. After cryoprotection with 30% (w/v) sucrose in 0.1 M PB, the brains were cut into frontal sections on a freezing microtome (CM1900, Leica). Free floating sections (30 μm thick) were incubated for over night at 37℃ in 0.1 M PB (pH 7.4) containing 0.5 mg/ml 3,3'-diaminobenzidine-4HCl (Dojindo), 0.15 mg/ml horse cytochrome c (Sigma), and 40 mg/ml

sucrose, and then rinsed in 0.01M PBS.

(5) Receptor autoradiography

Radiolabeled ligand binding for D1 class receptors and D2 class receptors were performed as described by Schambra et al. (1994) with minor modification. Mice were deeply anesthetized with sodium pentobarbital. The brains were quickly removed and cut into frontal sections on a freezing microtome (CM1900, Leica). For D1 class receptors, fresh-frozen sections (10 μm thick) were incubated for 30 min at room temperature in 50 mM Tris-HCl buffer (pH 7.4) containing 100 mM NaCl, 5 mM KCl, 2 mM $CaCl_2$, 1 mM $MgCl_2$ and 0.4 nM [^{3}H] SCH23390 (Perkin Elmer), and nonspecific binding was determined in the presence of 0.4 μM SCH23390 (Tocris Cookson). For D2 class receptors, the sections were incubated for 30 min at room temperature in 50 mM Tris-HCl buffer (pH 7.4) containing 140 mM NaCl and 1 nM [^{3}H] NMSP (Perkin Elmer), and nonspecific binding was determined in the presence of 1 μM spiperone (Sigma). The sections were then washed, dried, and expose to BAS-TR2040 imaging plates (Fuji Film).

Image analysis

Coronal sections through the dorsal striatum, GP, or STN were subjected to in situ hybridization, immunohistochemistry, CO histochemistry, and receptor autoradiography. Fifteen to twenty sections from each animal were used, and the anteroposterior coordinates (mm) from bregma were between 1.54 and –0.70 for the striatum, between –0.22 and –0.82 for the GP, and between –1.70 and –2.18 for the STN. For each section, a specified square (0.5 X 0.5 mm in the striatum and GP, and 0.1 X 0.1 mm in the STN) was selected on the corresponding region among comparison groups. Light microscopic images of brain sections

stained by in situ hybridization, immunohistochemistry or CO histochemistry were captured by the Zeiss AxioCam running on the AxioVision 3.0 software. Radiolabeled signals of in situ hybridization and receptor autoradiography were visualized by using BAS2500 Image Reader (Fuji Film). The number of stained neurons in the square was automatically counted with a computer-assisted imaging program (NIH Image 1.62) and the average of the neuronal number or the ratio of the neuronal number of IT-injected side relative to that on the PBS-injected side obtained from each animal was calculated. The intensity of histochemical signals in the square was measured with the same program. The activity of radiolabeled signals was measured by the BAS2500 Image Gauge (Fuji Film). The ratio of the radiolabeled activity of the IT-injected side relative to that on the PBS-injected side was calculated.

Neurochemical analysis

Contents of DA and its metabolites, including 3,4-dihydroxy-phenylacetic acid (DOPAC) and homovanillic acid (HVA), were measured according to the method described by Kobayashi et al. (1994) with slight modifications. Brains were rapidly removed and kept on ice while the striatum and the ventral midbrain were dissected. Dissected tissues were homogenized in 0.2 M perchloric acid containing 0.1 M EDTA and 1 μg/ml isoproterenol (Sigma). After centrifugation of the homogenates, the pH of the supernatant was adjusted to 3.0 by adding 1 M sodium acetate. The sample solutions (20 μl) were applied for a high-performance liquid chromatography equipped with electrochemical detection (HPLC-ECD) system (ECD300 series; SC-5ODS column, EICOM).

The mobile phase was 0.1 M sodium citrate, 0.1 M citric acid, 0.5 mM sodium octanesulfonate (Nacalai tesque), 0.15 mM EDTA, and 17% methanol (pH 3.5).

Behavioral analysis

(1) Rotational Behavior

For monitoring rotational behavior, mice were placed in a spherical bowl (25 cm in diameter), and the behavior was recorded with a digital video camera. One rotation was defined as a complete 360° turn. The number of rotations in the ipsilateral or contralateral directions was counted for every 10-min period by visual observation. Turning magnitude was defined as the total number of contralateral or ipsilateral rotations in a 30-min test period. Spontaneous turning magnitude was calculated during the pretreatment (-40 min to -10 min) and drug-induced turning magnitude was calculated after drug treatment (20 min to 50 min).

(2) Locomotor activity

Locomotor activity was measured with the movement analyzer (Scanet SV-10, Toyo Sangyo) using photo sensors as described (Nishii et al., 1998). Movement score was defined as the number of beam breaks for 10 min. Locomotor activity was defined as the total number of beam breaks in a 30-min test period. Spontaneous locomotor activity was measured during the pretreatment (-40 min to -10 min) and drug-induced locomotor activity was measured after drug treatment (20 min to 50 min).

After the behavioral testing, mice were deeply anesthetized with sodium pentobarbital, and brain sections were prepared. In situ hybridization analysis of the sections with the D2R probe confirmed the neuronal loss in the mutants treated with intrastriatal IT injection. Immunohistochemical analysis of brain sections with anti-choline acetyltransferase antibody confirmed the loss of striatal cholinergic interneurons in the mice treated with AF64A administration.

Drug Treatments

Methamphetamine sulfate (METH) was obtained from Dainippon Pharmaceutical Co., LTD. Apomorphine (APO), SKF81297 and Quinpirole hydrochloride (Quin) were obtained from Sigma. All drugs were freshly dissolved in 0.9% saline and injected *s.c.* or *i.p.* in a volume of 1.0 ml/kg .

Statistical analysis

For statistical comparisons, the ANOVA, Tukey-HSD test and Student's t test were used with significance set at $p < 0.05$. All values were expressed as the mean $\pm$ SEM of the data.

Results

Generation of mutant mice for targeting the D2R-expressing neurons

To express IL-2Rα under the control of the D2R gene, the knock-in approach was used. The IL-2Rα gene cassette was introduced into exon 2 of the mouse D2R locus with gene targeting in embryonic stem (ES) cells (Figure 1A and B). These ES clones were utilized to generate chimeric mice, which transmitted the mutation to their offspring. The expression pattern of IL-2Rα in mice heterozygous for the knock-in mutation was analyzed by in situ hybridization (Figure 1C). In the mutants, expression of the mRNA was detected in some brain regions including the striatum and ventral midbrain where endogenous D2R expression was detected, indicating the correct expression of the transgene under the control of the mouse D2R gene.

Ablation of D2R-expressing neurons in the striatum by IT injection

Mice heterozygous for the mutation were apparently normal in development and general behavior. In particular, they were normal in striatal structure, DA metabolism, and spontaneous and DA-induced motor behavior. Thus the wild type and heterozygous mutant littermates (8-16 weeks old) were utilized. To eliminate the striatal D2R-expressing neurons in the basal ganglia circuitry (Figure 2A), IT solution (5 ng/site) or 0.01 M phosphate-buffered saline (PBS) were unilaterally or bilaterally injected into six sites on one side of the dorsal striatum by a stereotaxic approach (see Figure 2B). In all experiments conducted in this study, the mice were used on day 7 after the injection.

Unilaterally injected mice were subjected to brain sectioning, and the sections through the striatum were stained with cresyl violet (Figure 2C). The number of stained neurons in the

striatum appeared to be moderately reduced on the IT-injected side in the mutants, on the other hand, there was no grossly visible damage on the IT-injected side in the wild types or on the PBS-injected sides in either type of mice. The sections through the striatum were analyzed by in situ hybridization with a riboprobe covering the D2R or D1R sequence (Figure 2D). Loss of D2R-expressing neurons was observed in the striatum of the IT-injected mutants. The neuronal loss was restricted in the dorsal region of the striatum, and it did not extend to the ventral region of the striatum. In contrast, D1R-expressing neurons were normally distributed in the striatum of the injected mutants. The number of neurons expressing D2R or D1R in the dorsal striatum was counted (Figure 2E). The number of D2R-expressing neurons was markedly reduced on the IT-injected side of the mutants ($p < 0.0001$), where the neuronal number was only 2.6% of that on the IT-injected side of the wild types. But it was not significantly different among PBS-injected side of the wild types, PBS-injected side of the mutants, and IT-injected side of the wild types. The number of D1R-expressing neurons was statistically indistinguishable among the four different injection sides. In addition, in situ hybridization analysis showed that the cortical neurons expressing D2R were intact in the injected mutants (Figure 2F). These results indicate a selective and efficient ablation of neuronal types expressing D2R in the dorsal striatum of the mutants by the IT injection.

The striatopallidal and striatonigral medium spiny neurons express enkephalin (ENK) and substance P (SP), respectively (Gerfen et al., 1990). Striatal GABAergic interneurons are divided into three categories that express parvalbumin, somatostatin, or calretinin (Kawaguchi et al., 1995). To determine the neuronal types in the D2R mutant mice affected by the IT injection, immunostaining was carried out with antibodies against specific markers for each neuronal type. For identification of the striatopallidal and striatonigral medium spiny neurons,

antibodies for a part of the precursor of ENK (preproenkephalin) or the precursor of SP (preprotachykinin A) was used respectively. The number of stained neurons on IT-injected side of the striatum was compared between the wild type and mutant mice (Figure 3). The number of neurons containing preproenkephalin was significantly reduced in the mutants ($p < 0.01$) to 8.9% of that found in the wild types. However, the number of preprotachykinin A-positive neurons was similar between the two genotypes. In addition, the number of cholinergic interneurons containing choline acetyltransferase was significantly decreased in the mutants ($p < 0.05$) to 30% of that of the wild types, whereas the numbers of the three categories of GABAergic interneurons were unaffected in the mutants. Thus the IT treatment of the mutants eliminated the majority of the striatopallidal medium spiny neurons and cholinergic interneurons, although the elimination of cholinergic interneurons was less than that of the striatopallidal medium spiny neurons.

Midbrain DA neuron morphology and DA metabolism in IT-injected mutants

In situ hybridization analysis of IL-2Rα expression in the D2R mutant mice showed the expression of transgene mRNA in the ventral midbrain (see Figure1C). Morphology of DA neurons in IT-injected or PBS-injected side of the brain was examined by immunohistochemistry with antibodies against tyrosine hydroxylase (TH) and DA transporter (DAT). The number of TH-positive neurons and the intensity of their immunoreactive signals in the SNc exhibited no visible changes in the IT-injected or the PBS-injected sides in either type of mice (Figure 4A). Distribution of the immunopositive fibers in the striatum was also unaffected in the IT-injected side of the mutants (Figure 4B). Staining with anti-DAT antibody confirmed a normal distribution of the nigrostriatal fibers in the same side of the

mutants (Figure 4C).

In addition, to examine influences of the intrastriatal IT injection in DA metabolism, the levels of DA and its metabolites, 3,4-dihydroxy-phenylacetic acid (DOPAC) and homovanillic acid (HVA) were examined in IT-injected or PBS-injected side of the striatum (Figure 5A) and the ventral midbrain (Figure 5B). Statistical analysis displayed no significant difference in the levels of DA, DOPAC, or HVA between the IT-injected or the PBS-injected sides in either type of mice. Consistent with the results obtained from histological experiments of the nigrostriatal DA pathway, these neurochemical data reveal that intrastriatal IT injection produced no apparent defects in DA metabolism in the IT-injected mutants.

Specific ligand binding for D2 and D1 class receptors in the dorsal striatum

Specific ligand binding for D2 and D1 class receptors in the dorsal striatum was analyzed. The sections prepared from unilaterally injected mice were subjected to receptor autoradiography with a D2 class receptor antagonist [^{3}H] NMSP or a D1 class receptor antagonist [^{3}H] SCH23390. The influence of IT injection on the number of ligand binding sites was evaluated as the relative ratio of activity of radiolabeled signals on the IT-injected side to that on the PBS-injected side (Figure 6). The ratio for D2 receptors in the mutants was reduced to 51% relative to that in the wild types ($p < 0.01$ according to Student's t test), whereas the ratio for D1 receptors was similar between the wild types and the mutants. The IT injection of the mutants led to a marked reduction in the number of D2 binding sites in the striatum but it apparently did not alter the number of D1 binding sites.

Ablation of striatal D2R-expressing neurons causes abnormal motor behavior

Asymmetry of basal ganglia output between both hemispheres is known to induce a turning behavior (Pycock, 1980). Unilateral treatments leading to suppression or activation of the output nuclei are generally thought to drive the movement contralateral or ipsilateral, respectively, to the treated side. To assess changes in basal ganglia output caused by ablation of the striatal D2R-expressing neurons, IT solution was injected unilaterally into the striatum, and then spontaneous and drug-induced turning behavior were tested. As shown in Figure 7A, the injected mutants displayed spontaneous turning in the direction contralateral to the injected side. After treatment with methamphetamine (METH, 6.0 mg/kg, *s.c.*), which stimulates DA release from presynaptic terminals, during the initial 20-min test period, the mutants reversed their turning (ipsilaterally). The ipsilateral turning reached a peak 30-40 min after treatment, and then was gradually attenuated. In contrast, the injected wild types exhibited a circling in neither the contralateral nor the ipsilateral direction. Turning magnitude defined as the total number of rotations in a 30-min test period during pretreatment or after drug treatment was measured (Figure 7B). Spontaneous turning magnitude during pretreatment in the contralateral direction was significantly increased in the mutants relative to that in the wild types ($p < 0.001$). The METH-induced turning magnitude in the ipsilateral direction after the treatment was significantly elevated in the mutants ($p < 0.01$). In addition, similar effects were observed after treatment with apomorphine (APO, 3.0 mg/kg, *s.c.*), which is non-selective DA receptor agonist (Figure 7C).

After treatment with SKF81297 (SKF, 4.8 mg/kg, *s.c.*), which is a D1 class-selective agonist, the contralateral rotations were significantly increased in the mutants ($p < 0.01$) (Figure 8A). After treatment of Quinpirole (Quin, 2.5 mg/kg, *s.c.*), which is a D2 class-

selective agonist, the contralateral rotations were reduced in the mutants but significantly exhibited contralateral circling relative to the wild type (Figure 8B). However, ipsilateral rotations were induced after treatment of both SKF and Quin in the mutants (Figure 8C).

These results suggest that the unilateral IT injection caused suppression of basal ganglia output on the injected side relative to that on the intact side (contralateral turning) in spontaneous movement, D1 class receptors stimulating state and D2 class receptors stimulating state. And the same injection produced an imbalance in suppression of the output nuclei in an opposite manner to the spontaneous movement (ipsilateral turning) in response to DA stimulation (both D1 and D2 class receptors stimulating state).

To further assess the changes in motor behavior derived from ablation of the D2R-expressing neurons, mice were bilaterally injected IT solution and monitored the spontaneous and METH-induced locomotion. Mice of both genotypes that received a bilateral sham operation with PBS displayed similar spontaneous and METH-induced locomotion (Figure 9A and 9B). As shown in Figure 9C, the IT injected mutants exhibited an increase in spontaneous movement score relative to the wild types throughout the pretreatment period. After METH treatment (2.0 mg/kg, *s.c.*), the movement score was remarkably elevated during the initial 10-min test period in both kinds of mice. In the wild types, the increase in the score lasted until 20-30 min after treatment. In the mutants the subsequent increase was moderate and attained a peak at a test period at 10-20 min. Locomotor activity was evaluated as the total number of movement score for 30 min before or after METH treatment (Figure 9D). Spontaneous locomotor activity during pretreatment was significantly increased in the mutants relative to that in the wild types ($p < 0.05$), being 2.3-fold of the wild type activity. After treatment, METH-induced locomotor activity in the wild types was markedly enhanced

to 8.2-fold of their basal activity. While the METH-induced locomotor activity in the mutants was increased to 2.7-fold of the mutant basal activity, and it was significantly lower than the corresponding value of the wild types (75%, $p < 0.01$). Bilateral neuronal elimination resulted in the hyperactivity in spontaneous locomotion, but impaired the motor activation in response to DA stimulation. These results agree with the data obtained from the turning behavior of the unilaterally IT-injected mutants, indicating the asymmetry of basal ganglia output between both hemispheres and the difference in rotational direction between before and after METH stimulation.

Ablation of the D2R-expressing neurons shifts gene expression in basal ganglia

An increase or decrease in the activity of striatonigral medium spiny neurons is known to upregulate or downregulate, respectively, the level of mRNA encoding SP (Gerfen et al., 1990). The level of mRNA encoding an isoform of glutamic acid decarboxylase (GAD67) is used to analyze changes in GABAergic activity in the GP neurons (Murer et al., 2000; Bacci et al., 2002). In addition, the activity of CO is an index of the metabolic activity of the STN neurons (Vila et al., 1996). To estimate the activity in basal ganglia neurons underlying the hyperactive spontaneous movement in IT-injected mutant mice, the expression levels of the above neuronal markers were investigated. SP mRNA in the dorsal striatum and GAD67 mRNA in the GP were detected by in situ hybridization, and CO activity in the STN was visualized by histochemistry. The effect of the IT injection on the expression levels was evaluated as the ratio of intensity on the IT-injected side relative to that on the PBS-injected side (Figure 10). The ratio of SP mRNA levels was not statistically distinguishable between the wild types and the mutants, whereas the ratio of GAD67 mRNA levels in the mutants was

1.2-fold higher than that in the wild types ($p < 0.01$ according to Student's t test). The ratio of CO activity in the mutants was mildly but significantly decreased to 93% of the wild type value ($p < 0.01$). These results suggest that the neuronal elimination influenced the spontaneous activity of the GP and STN neurons, while preserving the activity of the striatonigral medium spiny neurons at the normal level.

Administration of METH induces the expression of the immediate early gene c-*fos* in the striatum, GP, and STN (Graybiel et al., 1990; Cenci et al., 1992). In the striatum, c-*fos* expression is specifically induced in the striatonigral medium spiny neurons (Berretta et al., 1992; Cenci et al, 1992). To characterize the DA-dependent response of the basal ganglia neurons, c-*fos* expression in the basal ganglia after METH treatment (6.0 mg/kg, *i.p.*) was explored. The effect of IT injection in the gene expression was evaluated as the relative ratio of the number of c-*fos*-positive neurons on the IT-injected side to that on the PBS-injected side (Figure 11A). In the striatum, the ratio of the neuronal number was significantly attenuated in the mutants to 77% of the wild type value ($p < 0.01$, Student's t test). In contrast, the ratio in the GP was not statistically different between the wild types and the mutants. The ratio in the STN also resembled between the wild types and the mutants. These results suggest that the neuronal elimination impaired sufficient activation of the striatonigral medium spiny neurons in response to METH stimulation but that it did not apparently affect the activation of the GP and STN neurons.

METH stimulation also induces the expression of another IEG *zif268* in the striatum (Nguyen et al., 1992; Gerfen et al., 1995). To ascertain the effect of the neuronal ablation in METH-induced response of the striatonigral medium spiny neurons, the expression of *zif268* in the striatum after METH treatment (Figure 11B) was examined. The relative ratio of the

number of *zif268*-positive neurons on the IT-injected side to that on the PBS-injected side was reduced in the mutants to 76% of the wild type value ($p < 0.01$, Student's t test). The results agree with the data obtained from analysis of c-*fos* induction showing that the neuronal elimination attenuated upregulation of the striatonigral activity in response to METH stimulation.

D1 class receptors-mediated behavioral response

The attenuation in METH-induced c-*fos* and *zif268* expressions in the IT-injected striatum of the mutants suggests that elimination of the D2R-containing neurons may downregulate D1R-mediated cellular responsiveness of the striatonigral neurons. The behavioral response to a D1 class-selective agonist SKF81297 was tested. Bilaterally IT-injected mice were treated with low and high doses of SFK81297 (0.5 mg/kg and 2.0 mg/kg, *s.c.*) and then subjected to the behavioral analysis (Figure 12). Locomotor activity in the wild types showed 2.5-fold increase at the low dose and 3.6-fold increase at the high dose relative to the control activity treated with saline ($p < 0.01$). In the mutants, locomotor activity was again elevated in a dose-dependent manner similar to that in the wild types, and the increases were 1.8-fold at the low dose and 2.4-fold at the high dose relative to their control activity ($p < 0.01$). This data suggest a sparing of D1R-mediated cellular responsiveness of the striatonigral neurons in the IT-injected mutants.

Altered motor behavior is mainly caused by ablation of the striatopallidal neurons

In the striatum, ACh is reported to function to suppress locomotor activity through antagonizing DA actions via muscarinic receptor subtypes by inhibiting the striatonigral

medium spiny neurons and by stimulating the striatopallidal medium spiny neurons (Di Chiara et al., 1994; Wang and McGinity, 1997). Also, the ablation of striatal cholinergic interneurons eliminate ACh-mediated suppression of DA-induced hyperactivity (Kaneko et al., 2000). These data suggest that elimination of striatal cholinergic interneurons in the IT-injected mutant mice may contribute to the increased spontaneous movement. If the altered behavior were caused by the ablation of ACh functions, spontaneous locomotor activity would be expected to be increased by ablation of striatal cholinergic interneurons. Acetylethylcholine mustard aziridinium ion (acetyl AF64A), which is a selective cholinergic neurotoxin (Fisher et al., 1982) was administered intrastriatally. Immunohistochemical analysis with anti-choline acetyltransferase antibody indicated the reduction of the majority of cholinergic interneurons in AF64A-treated group (Figure 13A). The number of the positive neurons in the AF64A-treated group was 34% relative to that of the saline-treated group ($p < 0.01$). Mice bilaterally administered AF64A or saline were tested for locomotor activity (Figure 13B). Spontaneous locomotor activity was indistinguishable between the AF64A- and saline-treated groups. METH-induced locomotor activity exhibited a modest increase in the AF64A-treated group, being 1.2-fold higher than the saline-treated group ($p = 0.06$). In addition, c-*fos* induction in the striatum of unilaterally lesioned mice after METH treatment was examined (Figure 13C). The number of c-*fos*-positive neurons in the AF64A-treated side was 117% relative to that in the saline-treated side ($p < 0.05$). These results indicate that lesion of striatal cholinergic interneurons acted to enhance moderately METH-induced motor behavior with no apparent influence in spontaneous motor behavior, consistent with previous studies that show the role of cholinergic interneurons in suppression of DA-induced motor behavior (Di Chiara et al., 1994; Wang and McGinty, 1997; Kaneko et al., 2000).

Discussion

Functional analysis of the basal ganglia circuitry was based on lesion experiments of entire nuclei that constitute the circuitry. In the present study, IMCT technology was used to ablate specific neuronal types in the dorsal striatum for functional analysis of motor behavior. This approach provided a significant step forward in the understanding of basal ganglia physiology. Ablation of striatal neurons expressing the D2R subtype resulted in an elimination of the striatopallidal medium spiny neurons and cholinergic interneurons. The elimination of these neurons caused abnormalities in motor behavior, which were characterized by a hyperactivity of spontaneous movement and an attenuation of behavioral susceptibility to DA stimulation. The elimination also induced upregulation of GAD67 mRNA expression in the GP neurons and downregulation of CO activity in the STN neurons, whereas it attenuated DA-induced expression of the immediate early genes (IEGs) in the striatonigral medium spiny neurons. In addition, chemical lesion of cholinergic interneurons did not alter spontaneous movement but enhanced moderately in DA-induced motor activation. This enhancement of the behavior was accompanied by an increase in the IEGs expression in the striatonigral medium spiny neurons.

A selective localization of D1R in the striatonigral medium spiny neurons and D2R in the striatopallidal medium spiny neurons was reported in the previous histological studies (Gerfen et al., 1990; Hersch et al., 1995; Yung et al., 1995). However, colocalization of these subtypes in some identical spiny neurons was presented in other studies (Lester et al., 1993; Surmeier et al., 1996; Aizman et al., 2001). In the present study, IMCT of striatal D2R-expressing neurons eliminated the majority of striatopallidal medium spiny neurons with no influence on the number of striatonigral medium spiny neurons or D1R-expressing neurons

(Figure 2D). These results agree with the previous data reporting that the D1R and D2R subtypes are separately expressed in the different subpopulations of spiny neurons (Gerfen et al., 1990; Hersch et al., 1995; Yung et al., 1995). Among various types of striatal interneurons, IMCT of D2R-expessing neurons reduced the number of cholinergic interneurons (Figure 3), and the extent of the neuronal loss was 70%. This data support a previous study that subpopulations of striatal cholinergic interneurons expresses the D2R subtype (Aubry et al., 1993). In addition, the intrastriatal treatment of IT to the mutant mice produced no apparent damages on the morphology and DA metabolism in the nigrostriatal neurons in spite of the abundant expression of IL-2Rα (Figure 4, 5), indicating that DA neurons are resistant to IT molecules infused into their synaptic terminal regions. The resistance may be due to inefficiency of the receptor-mediated endocytosis from the synaptic terminals or retrograde axonal transport of IT molecules. Alternatively, the transgene products expressed in DA neurons may not be able to efficiently translocate to the terminal regions. Furthermore, IT injection of the mutants led to the reduction of approximately half the number of D2 binding sites in the striatum (Figure 6). The extent of the reduction is a consequence of ablation of the striatopallidal medium spiny neurons and cholinergic interneurons containing the D2R subtype. The remaining binding sites in the injected mutants may be derived from other D2 class receptor subtypes expressed in the intact striatal neurons or from the autoreceptor localized in the synaptic terminals of the nigrostriatal DA neurons.

In the standard model of the basal ganglia circuitry, the roles of the direct and indirect pathways have been considered to be implicated in activation and suppression of motor behavior, respectively (Alexander and Crutcher, 1990; DeLong, 1990; Gerfen and Wilson, 1996). At the striatal level, DA appears to facilitate the striatonigral medium spiny neurons

through the D1R subtype and to inhibit the striatopallidal medium spiny neurons through the D2R subtype (Gerfen and Wilson, 1996). The IT-injected mutant mice displayed the hyperactivity in spontaneous movement (Figure 9D), whereas chemical lesion of striatal cholinergic interneurons showed no apparent influence in the movement (Figure 13B). These behavioral data suggest that the spontaneous hyperactivity in the injected mutants is predominantly attributable to ablation of the striatopallidal medium spiny neurons. The spontaneous hyperactivity in the IT-injected mutants was accompanied by the increase in GAD67 mRNA level in the GP neurons and the decrease in CO activity in the STN neurons, with no apparent change in SP mRNA level in the striatonigral medium spiny neurons (Figure 10). These data suggest that the behavior is derived from modulation of neuronal activity in the indirect pathway. In particular, the elimination of the striatopallidal pathway may cause upregulation of the GP activity and downregulation of the STN activity, which reduce the net activity of basal ganglia output, thus leading to hyperactivity (see Figure 14A). These data suggest that the striatopallidal medium spiny neurons normally suppress spontaneous movement through inhibition of the GP neurons, in keeping with the role of the indirect pathway in the standard model of the circuitry.

On the other hand, the IT-injected mutant mice displayed a reduction in METH-induced motor behavior (Figure 9D), whereas chemical lesion of cholinergic interneurons caused a modest increase in METH-induced behavior (Figure 13B). The behavioral data suggest that the reduced motor behavior in the IT-injected mutants is mainly derived from ablation of the striatopallidal medium spiny neurons. The impairment in METH-induced motor activation observed in IT-injected mutants dose not simply results from removal of the suppression of motor behavior by the indirect pathway according to the standard model of the basal ganglia

circuitry. In addition, the IT injection of the mutants attenuated METH-induced IEGs expression in the striatonigral medium spiny neurons, although, retaining a normal level of D1 class receptor binding (Figure 6), D1 class receptor-mediated locomotor activity (Figure 12) and the IEG expression in the GP and STN (Figure 11A). Lesion of cholinergic interneurons slightly increased the IEG expression in the striatonigral medium spiny neurons (Figure 13C). The comparison of IEG expression levels in the striatonigral medium spiny neurons between IT-injected mutant and chemically-lesioned mice suggests that the attenuated IEGs expression in the injected mutants is mostly linked to the ablation of the striatopallidal medium spiny neurons. Taken together, these data suggest that the presence of an additional mechanism that enhance the striatonigral activity in response to DA stimulation through the striatopallidal medium spiny neurons. Elimination of the striatopallidal medium spiny neurons reduces DA-induced motor activation at least in part through the insufficient activation of the striatonigral medium spiny neurons, which inhibits a normal suppression of the basal ganglia output (see Figure 14B and14C). The striatopallidal medium spiny neurons appear to be involved in full expression of DA-induced behavior not only through the disinhibition of the GP neurons but also through the facilitation of the striatonigral medium spiny neurons. Although the precise mechanism by which the striatopallidal medium spiny neurons affect the striatonigral medium spiny neurons is not clear.

One possible mechanism for the regulation of the striatonigral medium spiny neurons in response to DA transmission through the striatopallidal medium spiny neurons is modulation of inhibitory transmission via local axon collaterals of medium spiny neurons within the striatal circuitry. Spiny neurons extend the axon collaterals that make synaptic contact with other striatal neurons (Wilson and Groves, 1980). Although a previous study failed to detect

mutual electrophysiological responses between spiny neurons (Jaeger et al., 1994), recent reports showed that these neurons are interconnected by GABAergic synaptic transmission (Czubayko and Plenz, 2002; Tunstall et al., 2002). Spiny neurons also receive synaptic inputs from some types of GABAergic interneurons (Kawaguchi, 1993; Koós and Tepper, 1999; Kubota and Kawaguchi, 2000). These observations suggest that D2R-mediated inhibition of the striatopallidal medium spiny neurons may subserve D1R-mediated facilitation of the striatonigral medium spiny neurons through axonal interactions between spiny neurons or through the interneuronal network. The D2R-mediated inhibition may need to be temporally coupled to the D1R-mediated facilitation to express an adequate response of the striatonigral medium spiny neurons, as observed in many DA actions requiring synergistic effects between D1 class and D2 class receptors (Walters et al., 1997; LaHoste et al., 1993; Gerfen et al., 1995). Another possible mechanism may involve the function of ENK that inhibits the striatonigral activity. ENK is reported to depress D1 class receptor-mediated cAMP signal transduction in the striatal slices (Schoffelmeer et al., 1993; Lindskog et al., 1999). Also, the mRNA encoding μ-opioid receptors appears to be localized in the majority of striatonigral medium spiny neurons in the striosomal patch compartments (Guttenberg et al., 1996). These data suggest that DA-dependent reduction in ENK levels may trigger the facilitation of the striatonigral activity. The detailed neural mechanism that controls the striatonigral activity in response to DA transmission through the striatopallidal medium spiny neurons remains to be determined.

Pharmacological blockade of D2 receptors is generally known to produce a decrease in locomotor activity (Jackson et al., 1994). Disruption of the mouse D2R gene causes locomotor impairment (Baik et al., 1995). Although these studies showed that D2R-mediated

signaling plays a key role in motor control, the mechanism by which the signaling regulates the basal ganglia circuitry has not been fully elucidated. In the present study, IMCT strategy ablated specific neuronal types expressing D2R in the striatum and demonstrated an important role of the striatopallidal medium spiny neurons in dual regulation of basal ganglia function through coordination of the direct and indirect pathways. These neurons suppress spontaneous motor behavior through inhibition of the GP. In response to DA stimulation, they act to fully express motor activation not only through disinhibition of the GP but also through facilitation of the striatonigral medium spiny neurons. An understanding of the molecular and cellular mechanisms for the coordination of the neural pathways should provide new directions to elucidate the physiological basis of various psychomotor functions mediated by the basal ganglia. In addition, Parkinson's disease, which is caused by selective degeneration of midbrain DA neurons, is thought to reflect a disturbance in basal ganglia function. One therapeutic approach to improve the motor symptoms of the disease is high-frequency stimulation of deep brain regions, but the basis of the clinical efficacy is unknown. A better understanding of the mechanism that operates the basal ganglia circuitry will be of importance to elucidate the pathological conditions of Parkinson's disease and to provide scientific support for the therapeutic approach of the disease.

Finally, IMCT technology enabled to perform functional analysis of the basal ganglia circuitry by ablating specific neuronal types expressing D2R from the striatal neural network. The results in the present study provide evidence that the striatopallidal medium spiny neurons play an important role in dual regulation of motor behavior depending on the state of DA transmission via coordination of the direct and indirect pathways. In particular, the impairment of DA-induced motor activation observed in the IT-injected mutants does not

simply result from removal of the suppression of motor behavior by the indirect pathway according to the standard model of the basal ganglia circuitry. The data suggest the presence of an additional mechanism that facilitates the motor behavior in response to DA stimulation through the striatopallidal medium spiny neurons. Understanding molecular and neuronal mechanisms for the neural circuit coordination should help to elucidate the physiological basis of various psychomotor functions mediated by the basal ganglia as well as the pathological conditions of the disorders associated with disturbance in the basal ganglia.

Acknowledgements

First, and foremost, I would like to thank Dr. Kazuto Kobayashi for giving me the opportunity to study this theme in the Department of Molecular Genetics, Fukushima Medical University, and for a lot of helpful and critical discussions.

I would also like to thank Dr. Kenji Kohno for allowing me to study in the Department of Molecular Genetics, Fukushima Medical University, Dr. Yasunobu Yasoshima for teaching me the statistical analysis and a lot of helpful discussions, Dr. Natsuki Matsushita and Mr. Kenta Kobayashi for teaching me the basis of molecular biology.

In addition, I would like to thank the following:

To Dr. Takeshi Kaneko for a lot of helpful discussions and providing the antibody against preproenkephalin and preprotachykinin A.

To Dr. Ira Pastan for providing the recombinant immunotoxin anti-Tac(Fv)-PE38.

To Drs. Toshiharu Nagatsu, Hirohide Sawada, Kazuhiro Nishii and Ms. Michiko Saito for generation of the mutant mice.

To Dr. Hitoshi Kawano for providing the antibody against choline acetyltransferase.

To Drs. Shigetada Nakanishi and Satoshi Kaneko for providing the D2R and SP cDNA.

To Dr. Uchio Yanagawa for providing the GAD67 cDNA.

To Mr. Hideki Okada and Ms. Minako Kikuchi for technical support.

References

Aizman, O., Brismar, H., Uhlen, P., Zettergren, E., Levey, A.I., Forssberg, H., Greengard, P., and Aperia, A. (2000). Anatomical and physiological evidence for D1 and D2 dopamine receptor colocalization in neostriatal neurons. Nature Neuroscience 3, 226-230.

Alexander, G. E., and Crutcher, M. D. (1990). Functional architecture of basal ganglia circuits: neural substrates of parallel processing. Trends in Neurosciences 13, 266-271.

Aubry, J-M., Schulz, M-F., Pagliusi, S., Schultz, P., and Kiss, J.Z. (1993). Coexpression of dopamine D_2 and substance P (neurokinin-1) receptor messenger RNAs by a subpopulation of cholinergic neurons in the rat striatum. Neuroscience 53, 417-424.

Bacci, J-J., Goff, L. K-L., and Salin, P. (2002). Effects of intralaminar thalamic nuclei lesion on glutamic acid decarboxylase (GAD65 and GAD67) and cytochrome oxidase subunit I mRNA expression in the basal ganglia of the rat. European Journal of Neuroscience 15, 1918-1928.

Baik, J. -H., Picetti, R., Dalardi, A., Thirlet, G., Dierich, A., Le Meur, M., and Borelli, E. (1995). Parkinsonian-like locomotor impairment in mice lacking dopamine D2 receptors. Nature 377, 424-428.

Bergman, H., Feingold, A., Nini, A., Raz, A., Slovin, H., Abeles, M., and Vaadia, E. (1998). Physiological aspects of information processing in the basal ganglia of normal and parkinsonian primates. Trends in Neuroscience 21, 32-38.

Berretta, S., Robertson, H. A., and Graybiel, A. M. (1992). Dopamine and glutamate agonists stimulate neuron-specific expression of Fos-like protein in the striatum. Journal of Neurophysiology 68, 767-777.

Bevan, M.D., Magill, P. J., Terman, D., Bolam, J. P., and Wilson, C. J. (2002). Move to the rhythm: oscillations in the subthalamic nucleus-external globus pallidus network. Trends in Neuroscience 25, 525-531.

Cenci, M. A., Kalen, P., Mandel, R. J., Wictorin, K., and Bjorklund, A. (1992). Dopaminergic transplants normalize amphetamine- and apomorphine-induced Fos expression in the 6-hydroxydopamine-lesioned striatum. Neuroscience 46, 943-957.

Civelli, O., Bunzow, J. R., and Grandy, D. K. (1993). Molecular diversity of the dopamine receptors. Annual Review of Pharmacology & Toxicology 33, 281-307.

Czubayko, U., and Plenz, D. (2002). Fast synaptic transmission between striatal spiny projection neurons. Proceedings of the National Academy of Sciences of the United States of America 99, 15764-15769.

DeLong, M. R. (1990). Primate models of movement disorders of basal ganglia origin. Trends in Neurosciences 13, 281-285.

Di Chiara, G., Morelli, M., and Consolo, S. (1994). Modulatory functions of neurotransmitters in the striatum: ACh/dopamine/NMDA interactions. Trends in Neurosciences 17, 228-233.

Drago, J., Gerfen, C. R., Lachowicz, J. E., Steiner, H., Hollon, T. R., Love, P. E., Ooi, G. T., Grinberg, A., Lee, E. J., Huang, S. P., Bartlett, P. F., Jose, P. A., Sibley, D. R., and Westphal, H. (1994). Alterd striatal function in a mutant mouse lacking D1A dopamine receptors. Proceedings of the National Academy of Sciences of the United States of America 91, 12546-12568

Fisher, A., Mantione, C. R., Abraham, D. J., and Hanin, I. (1982). Long-term central cholinergic hypofunction induced in mice by ethylcholine azirizium ion (AF64A) *in vivo*.

Journal of Pharmacology & Experimental Therapeutics 222, 140-145.

Gerfen, C. R., and Wilson. C. J. (1996). The basal ganglia. In Handbook of Chemical Anatomy, Integrated Systems in the CNS, Part III, Swanson L. W. et al., ed. (Elsevier), pp. 371-468.

Gerfen, C. R. (1992a). The neostriatal mosaic: multiple levels of compartmental organization. Trends in Neurosciences 15, 133-139.

Gerfen, C. R. (1992b). The neostriatal mosaic: multiple levels of compartmental organization in the basal ganglia. Annual Review of Neuroscience 15, 285-320.

Gerfen, C. R., Keefe, K. A., and Gauda, E. B. (1995). D1 and D2 dopamine receptor function in the striatum: coactivation of D1- and D2-dopamine receptors on separate populations of neurons results in potentiated immediate early gene response in D1-containing neurons. Journal of Neuroscience 15, 8167-8176.

Gerfen, C. R., Engber, T. M., Mahan, L. C., Susel, Z., Chase, T. N., Monsma, F. J., Jr., and Sibley, D. R. (1990). D1 and D2 dopamine receptor-regulated gene expression of striatonigral and striatopallidal neurons. Science 250, 1429-1432.

Gingrich, J. A., and Caron, M. G. (1993). Recent advances in the molecular biology of dopamine receptors. Annual Review of Neuroscience 16, 299-321.

Graybiel, A. M. (1995). Building action repertoires: memory and learning functions of the basal ganglia. Current Opinion in Neurobiology 5, 733-741.

Graybiel, A. M., Aosaki, T., Flaherty, A. W., and Kimura, M. (1994). The basal ganglia and adaptive motor control. Science 265, 1826-1831.

Graybiel, A. M., Moratalla, R., and Robertson, H. A. (1990). Amphetamine and cocaine induce drug-specific activation of the c-fos gene in striosome-matrix compartments and

limbic subdivisions of the striatum. Proceedings of the National Academy of Sciences of the United States of America 87, 6912-6916.

Guttenberg, N. D., Klop, H., Minami, M., Satoh, M., and Voorn, P. (1996). Co-localization of mu opioid receptor is greater with dynorphin than enkephalin in rat striatum. NeuroReport 7, 2119-2124.

Hersch, S. M., Ciliax, B. J., Gutekunst, C. A., Rees, H. D., Heilman, C. J., Yung, K. K., Bolam, J. P., Ince, E., Yi, H., and Levey, A. I. (1995). Electron microscopic analysis of D1 and D2 dopamine receptor proteins in the dorsal striatum and their synaptic relationships with motor corticostriatal afferents. Journal of Neuroscience 15, 5222-5237.

Hikida, T., Kaneko, S., Isobe, T., Kitabatake, Y., Watanabe, D., Pastan, I., and Nakanishi, S. (2001). Increased sensitivity to cocaine by cholinergic cell ablation in nucleus accumbens. Proceedings of the National Academy of Sciences of the United States of America 98, 13351-13354.

Hikida, T., Kitabatake, Y., Pastan, I., and Nakanishi, S. (2003). Acetylcholine enhancement in the nucleus accumbens prevents addictive behaviors of cocaine and morphine. Proceedings of the National Academy of Sciences of the United States of America 100, 6169-6173.

Ichikawa, T., Ajiki, K., Matsuura, J., and Misawa, H. (1997). Localization of two cholinergic markers, choline acetyltransferase and vesicular acetylcholine transporter in the central nervous system of the rat: in situ hybridization histochemistry and immunohistochemistry. Journal of Chemical Neuroanatomy 13, 23-39.

Jaeger, D., Kita, H., and Wilson, C. J. (1994). Surround inhibition among projection neurons

is weak or nonexistent in the rat neostriatum. Journal of Neurophysiology 72, 2555-2558.

Jackson, D. M., Westlind-Danielsson, A. (1994). Dopamine receptors: molecular biology, biochemistry and behavioral aspects. Pharmacological Therapeutics 64, 291-369.

Kaneda, N., Sasaoka, T., Kobayashi, K., Kiuchi, K., Nagatsu, I., Kurosawa, Y., Fujita, K., Yokoyama, M., Nomura, T., and Katsuki, M. (1991). Tissue-specific and high-level expression of the human tyrosine hydroxylase gene in transgenic mice. Neuron 6, 583-594.

Kaneko, S., Hikida, T., Watanabe, D., Ichinose, H., Nagatsu, T., Kreitman, R. J., Pastan, I., and Nakanishi, S. (2000). Synaptic integration mediated by striatal cholinergic interneurons in basal ganglia function. Science 289, 633-637.

Kawaguchi, Y. (1993). Physiological, morphological, and histochemical characterization of three classes of interneurons in rat neostriatum. Journal of Neuroscience 13, 4908-4923.

Kawaguchi, Y., Wilson, C. J., Augood, S. J., and Emson, P. C. (1995). Striatal interneurones: chemical, physiological and morphological characterization. Trends in Neurosciences 18, 527-535.

Kimura, M. (1995). Role of basal ganglia in behavioral learning. Neuroscience Research - Supplement 22, 353-358.

Kitabatake, Y., Hikida, T., Watanabe, D., Pastan, I., and Nakanishi, S. (2003). Impairment of reward-related learning by cholinergic cell ablation in the striatum. Proceedings of the National Academy of Sciences of the United States of America 100, 7965-7970.

Kobayashi, K., Morita, S., Sawada, H., Mizuguchi, T., Yamada, K., Nagatsu, I., Fujita, K., Kreitman, R. J., Pastan, I., and Nagatsu, T. (1995a). Immunotoxin-mediated conditional

disruption of specific neurons in transgenic mice. Proceedings of the National Academy of Sciences of the United States of America 92, 1132-1136.

Kobayashi, K., Morita, S., Sawada, H., Mizuguchi, T., Yamada, K., Nagatsu, I., Hata, T., Watanabe, Y., Fujita, K., and Nagatsu, T. (1995b). Targeted disruption of the tyrosine hydroxylase locus results in severe catecholamine depletion and perinatal lethality in mice. Journal of Biological Chemistry 270, 27235-27243.

Kobayashi, K., Ohye, T., Pastan, I., and Nagatsu, T. (1996). A novel strategy for the negative selection in mouse embryonic stem cells operated with immunotoxin-mediated cell targeting. Nucleic Acids Research 24, 3653-3655.

Kobayashi, K., Morita, S., Mizuguchi, T., Sawada, H., Yamada, K., Nagatsu, I., Fujita, K., and Nagatsu, T. (1994). Functional and high level expression of human dopamine beta-hydroxylase in transgenic mice. Journal of Biological Chemistry 269, 29725-29731.

Koós, T., and Tepper, J. M. (1999). Inhibitory control of neostriatal projection neurons by GABAergic interneurons. Nature Neuroscience 2, 467-472.

Kreitman, R. J., Bailon, P., Chaudhary, V. K., FitzGerald, D. J., and Pastan, I. (1994). Recombinant immunotoxins containing anti-Tac(Fv) and derivertives of Pseudomonas exotoxin produce complete regression in mice of an interleukin-2 receptor-bearing human carcinoma. Blood 83, 426-434.

Kubota, Y., and Kawaguchi, Y. (2000). Dependence of GABAergic synaptic areas on the interneuron type and target size. Journal of Neuroscience 20, 375-386.

LaHoste, G. J., Yu, J., and Marshall, J. F. (1993). Striatal Fos expression is indicative of dopamine D1/D2 synergism and receptor supersensitivity. Proceedings of the National Academy of Sciences of the United States of America 90, 7451-7455.

Lee, T., Kaneko, T., Taki, K., and Mizuno, N. (1997). Preprodynorphin-, preproenkephalin-, and preprotachykinin-expressing neurons in the rat neostriatum: an analysis by immunocytochemistry and retrograde tracing. Journal of Comparative Neurology 386, 229-244.

Lester, J., Fink, S., Aronin, N., and DiFiglia, M. (1993). Colocalization of D1 and D2 dopamine receptor mRNAs in striatal neurons. Brain Research 621, 106-110.

Lindskog, M., Svenningsson, P., Fredholm, B., Greengard, P., and Fisone, G. (1999). Mu- and delta-opioid receptor agonists inhibit DARPP-32 phosphorylation in distinct populations of striatal projection neurons. European Journal of Neuroscience 11, 2182-2186.

Maldonado, R., Saiardi, A., Valverde, O., Samad, T. A., Roques, B. P., and Borrelli, E. (1997). Nature 388, 586-589.

Murer, M. G., Dziewczapolski, G., Salin, P., Vila, M., Tseng, K. Y., Ruberg, M., Rubinstein, M., Kelly, M. A., Grandy, D. K., Low, M. J., Hirsch, E., Raisman-Vozari, R., and Gershanik, O. (2000). The indirect basal ganglia pathway in dopamine D(2) receptor-deficient mice. Neuroscience 99, 643-650.

Nambu, A., Tokuno, H., and Takada, M. (2002). Functional significance of the cortico-subthalamo-pallidal 'hyperdirect' pathway. Neuroscience Research 43, 111-117.

Nguyen, T.V., Kosofsky, B.E., Birnbaum, R, Cohen, B. M., and Hyman, S.E. (1992). Differential expression of c-Fos and Zif268 in rat striatum after haloperidol, clozapine, and amphetamine. Proceedings of the National Academy of Sciences of the United States of America 89, 4270-4274.

Nicola, S. M., Surmeier, J., and Malenka, R. C. (2000). Dopaminergic modulation of neuronal excitability in the striatum and nucleus accumbens. Annual Review of Neuroscience 23,

185-215.

Nishii, K., Matsushita, N., Sawada, H., Sano, H., Noda, Y., Mamiya, T., Nabeshima, T., Nagatsu, I., Hata, T., Kiuchi, K., Yoshizato, H., Nakashima, K., Nagatsu, T., and Kobayashi, K. (1998). Motor and learning dysfunction during postnatal development in mice defective in dopamine neuronal transmission. Journal of Neuroscience Research 54, 450-464.

Parent, A., and Hazrati, L. N. (1995). Functional anatomy of the basal ganglia. I. The cortico-basal ganglia-thalamo-cortical loop. Brain Research - Brain Research Reviews 20, 91-127.

Paxinos, G., and Franklin, K. B. J. (2001). The Mouse Brain in Stereotaxic Coordinates, (San Diego: Academic Press).

Pycock, C. J. (1980). Turning behaviour in animals. Neuroscience 5, 461-514.

Rinne, J. O. (1993). Nigral degeneration in Parkinson's disease. Movement Disorders 8, Suppl 1, S31-35.

Roberts, R. C., Harrison, M. B., Francis, S. M., and Wiley, R. G. (1993). Differential effects of suicide transport lesions of the striatonigral or striatopallidal pathways on subsets of striatal neurons. Experimental Neurology 124, 242-252.

Sawada, H., Nishii, K., Suzuki, T., Hasegawa, K., Hata, T., Nagatsu, I., Kreitman, R. J., Pastan, I., Nagatsu, T., and Kobayashi, K. (1998). Autonomic neuropathy in transgenic mice caused by immunotoxin targeting of the peripheral nervous system. Journal of Neuroscience Research 51, 162-173.

Schambra, U.B., Duncan, G.E., Breese, G.R., Fornaretto, M.G., Caron, M.G., and Fremeau, Jr. R.T. (1994). Ontogeny of D1A and D2A dopamine receptor subtypes in rat brain using in

situ hybridization and receptor binding. Neuroscience 62, 65-85.

Schoffelmeer, A. N., De Vries, T. J., Hogenboom, F., and Mulder, A. H. (1993). Mu- and delta-opioid receptors inhibitorily linked to dopamine-sensitive adenylate cyclase in rat striatum display a selectivity profile toward endogenous opioid peptides different from that of presynaptic mu, delta and kappa receptors. Journal of Pharmacology & Experimental Therapeutics 267, 205-210.

Schultz, W., Dayan, P., and Montague, P. R. (1997). A neural substrate of prediction and reward. Science 275, 1593-1599.

Surmeier, D. J., Song, W. J., and Yan, Z. (1996). Coordinated expression of dopamine receptors in neostriatal medium spiny neurons. Journal of Neuroscience 16, 6579-6591.

Szczypka, M. S., Mandel, R. J., Donahue, B. A., Snyder, R. O., Leff, S. E., and Palmiter, R. D. (1999a). Viral gene delivery selectively restores feeding and prevents lethality of dopamine-deficient mice. Neuron 22, 167-178.

Szczypka, M. S., Rainey, M. A., Kim, D. S., Alaynick, W. A., Marck, B. T., Matsumoto, A. M., and Palmiter, R. D. (1999b). Feeding behavior in dopamine-deficient mice. Proceedings of the National Academy of Sciences of the United States of America 96, 12138-12143.

Szczypka, M. S., Kwok, K., Brot, M. D., Marck, B. T., Matsumoto, A. M., Donahue, B. A., and Palmiter, R. D. (2001). Dopamine production in the caudate putamen restores feeding in dopamine-deficient mice. Neuron 30, 819-828.

Tunstall, M. J., Oorschot, D.E., Kean, A,. and Wickens, J. R. (2002). Inhibitory interactions between spiny projection neurons in the rat striatum. Journal of Neurophysiology 88, 1263-1269.

Vila, M., Levy, R., Herrero, M. T., Faucheux, B., Obeso, J. A., Agid, Y., and Hirsch, E. C. (1996). Metabolic activity of the basal ganglia in parkinsonian syndromes in human and non-human primates: a cytochrome oxidase histochemistry study. Neuroscience 71, 903-912.

Walters, J. R., Bergstrom, D. A., Carlson, J. H., Chase, T. N., and Braun, A. R. (1987). D1 dopamine receptor activation required for postsynaptic expression of D2 agonist effects. Science 236, 719-722.

Wang, J. Q., and McGinty, J. F. (1997). Intrastriatal injection of a muscarinic receptor agonist and antagonist regulates striatal neuropeptide mRNA expression in normal and amphetamine-treated rats. Brain Research 748, 62-70.

Watanabe, D., Inokawa, H., Hashimoto, K., Suzuki, N., Kano, M., Shigemoto, R., Hirano, T., Toyama, K., Kaneko, S., Yokoi, M., Moriyoshi, K., Suzuki, M., Kobayashi, K., Nagatsu, T., Kreitman, R. J., Pastan, I., and Nakanishi, S. (1998). Ablation of cerebellar Golgi cells disrupts synaptic integration involving GABA inhibition and NMDA receptor activation in motor coordination. Cell 95, 17-27.

Weick, B. G., and Walters, J. R. (1987). Effects of D1 and D2 dopamine receptor stimulation on the activity of substantia nigra pars reticulata neurons in 6-hydroxydopamine lesioned rats: D1/D2 coactivation induces potentiated responses. Brain Research 405, 234-246.

Wickens, J. (1990). Striatal dopamine in motor activation and reward-mediated learning: steps towards a unifying model. Journal of Neural Transmission - General Section 80, 9-31.

Wilson, C. J., and Groves, P. M. (1980). Fine structure and synaptic connections of the common spiny neuron of the rat neostriatum: a study employing intracellular inject of horseradish peroxidase. Journal of Comparative Neurology 194, 599-615.

Xu, M., Moratalla, R., Gold, L. H., Hiroi, N., Koob, G. F., Graybiel, A. M., and Tonegawa, S. (1994a). Dopamine D1 receptor mutant mice are deficient in striatal expression of dynorphin and in dopamine-mediated behavior responses. Cell 79, 729-742

Xu, M., Hu, X. -T., Cooper, D. C., Moratalla, R., Graybiel, A. M., White, F. J., and Tonegawa, S. (1994b). Elimination of cocaine-induced hyperactivity and dopamine-mediated neurophysiological effects in dopamine D1 receptor mutant mice. Cell 79, 945-955

Yoshida, K., Watanabe, D., Ishikane, H., Tachibana, M., Pastan, I., and Nakanishi, S. (2001). A key role of starburst amacrine cells in originating retinal directional selectivity and optokinetic eye movement. Neuron 30, 771-780.

Young, R. (1999). Update on Parkinson's disease. American Family Physician 59, 2155-2167.

Yung, K. K., Bolam, J. P., Smith, A. D., Hersch, S. M., Ciliax, B. J., and Levey, A. I. (1995). Immunocytochemical localization of D1 and D2 dopamine receptors in the basal ganglia of the rat: light and electron microscopy. Neuroscience 65, 709-730.

Zhou, Q. Y., and Palmiter, R. D. (1995). Dopamine-deficient mice are severely hypoactive, adipsic, and aphagic. Cell 83, 1197-1209.

Figure Legends

Figure 1. Mutant mice expressing IL-2Rα under the control of the D2R gene.

(A) Strategy for the knock-in mutagenesis. The targeting vector contains the 5'-homologous region, the human IL-2Rα gene cassette fused to the polyadenylation signal (PA), the phosphoglycerate kinase-1-*neo* gene cassette (neo), the 3'-homologous region, and the diphtheria toxin A-fragment (DTA) gene cassette. The restriction enzyme fragments for Southern blotting with probes A, B and C are indicated. A, *Apa*I; B, *Bam*HI; Bs, *Bst*PI; E, *Eco*RI; H, *Hin*dIII; S, *Sph*I; and PA, Polyadenylation signal. (B) Genotyping of ES cellular DNA. Genomic DNA from a representative ES clone carrying the targeted mutation and from wild type cells were digested with the indicated restriction enzymes and subjected to Southern blotting with probe A, B or C. (C) In situ hydridization analysis of IL-2Rα expression. Coronal brain sections were used for in situ hybridization with ^{35}S-labeled riboprobe for a mouse D2R or human IL-2Rα sequence. ST, striatum; NAc, nucleus accumbens; OT, olfactory tubercle; VTA, ventral tegmental area. Scale bar, 1 mm.

Figure 2. Elimination of the striatal D2R-expressing neurons by IT injection.

(A) Model of the basal ganglia circuitry. The excitatory and inhibitory transmission pathways are illustrated by lines terminating with triangles and bars, respectively. EPN, entopeduncular nucleus; ST, striatum. (B) Schematic illustration of coordinates for the intrastriatal injection. (C) Nissl staining of coronal brain sections through the striatum prepared from mice unilaterally injected with IT solution or PBS. Scale bar, 25 μm. (D) In situ hybridization analysis of the D2R- and D1R-expressing neurons in the striatum. The sections (10 μm thick) were hybridized with digoxygenin-labeled riboprobe for a mouse D2R or D1R sequence.

Light microscopic images of the IT-injected side of the striatum in the wild type and mutant mice are shown. Lower panels show 6-fold magnified views of the dorsal region of the striatum. The dorsal (D) and ventral (V) regions of the striatum are indicated. ac, anterior commissure. Scale bar, 200 μm. (E) Number of striatal neurons expressing D2R or D1R. The neuronal number in the specified areas in the dorsal striatum (0.5 X 0.5 mm) was counted. Open column, wild type mice (n = 4); closed column, mutant mice (n = 4). $*p < 0.0001$, significant difference from the IT-injected wild type mice (Tukey-HSD test). (F) D2R in situ hybridization of the sections through the frontal cortex prepared from mice that received the intrastriatal IT injection. Arrows show the representative neurons displaying the hybridization signals. Scale bar, 20 μm.

Figure 3. Typing of the neuronal populations affected by IT injection.

The sections (30 μm thick) were immunohistochemically stained for specific markers of the striatal neuronal populations. Striatopallidal and striatonigral medium spiny neurons were labeled for preproenkephalin (PPE) and preprotachykinin A (PPT), respectively; and cholinergic interneurons, by that for choline acetyltransferase (ChAT). The three kinds of GABAergic interneurons were labeled with antibodies for parvalbumin (PV), somatostatin (SS), or calretinin (CR). Open column, wild type mice (n = 4); closed column, mutant mice (n = 4). $*p < 0.01$, $**p < 0.05$, significant differences from the wild type mice (Student's *t* test). Light microscopic images of the representative sections are indicated. Scale bar, 50 μm.

Figure 4. Morphology of the nigrostriatal DA neurons.

Histology of DA neurons stained with antibodies for TH (A and B) or DAT (C). Light

microscopic images for the IT-injected or PBS-injected sides of the SNc and the striatum are indicated for the TH staining; and those for the IT-injected side of the striatum, for the DAT staining. Scale bar, 100 μm (A), 500 μm (B and C).

Figure 5. Metabolism of the nigrostriatal DA neurons.

Contents of DA, DOPAC, and HVA in the striatum (A) and ventral midbrain (B) with the IT-injected or PBS-injected mice. Open column, wild type mice (n = 5); closed column, mutant mice (n = 5).

Figure 6. Binding site of D2 and D1 class receptors in the striatum.

Radiolabeled ligand binding of D2 and D1 class receptors in the striatum. The value is expressed as the ratio of the intensity of binding signals on the IT-injected side relative to that on the PBS-injected side. Open column, wild type mice (n = 6); closed column, mutant mice (n = 6). $*p < 0.01$, significant differences from the wild type mice according to Student's *t* test.

Figure 7. Spontaneous and DA-induced rotational behavior.

(A) Time course of turning behavior of mice unilaterally injected with IT solution. After monitoring of spontaneous rotation for 1 hr, the mice were administered METH (6.0 mg/kg, *s.c.*). The number of rotations in the ipsilateral (ipsi) or contralateral (contra) direction was counted for 10-min periods. (B-C) Turning magnitude. The total number of contralateral or ipsilateral rotations in a 30-min test period was calculated to evaluate spontaneous turning magnitude and METH (B) or apomorphine (APO, 2.0 mg/kg, *s.c.*) (C) -induced turning

magnitude. Wild type mice (n = 5); Mutant mice (n = 6). *$p < 0.001$ versus the wild type spontaneous magnitude; **$p < 0.01$ versus the wild type drug-induced magnitude, significant differences according to the Tukey-HSD test.

Figure 8. Selective DA receptor agonists-induced rotational behavior.

The total number of contralateral or ipsilateral rotations in a 30-min test period was calculated to evaluate SKF81297 (SKF, 4.8 mg/kg, *s.c.*) (A), Quinpirole (Quin, 2.5 mg/kg, *s.c.*) (B) and both SKF and Quin (C) -induced turning magnitude. Wild type mice (n = 4); Mutant mice (n = 4). *$p < 0.01$ versus the wild type drug-induced magnitude, significant differences according to the Tukey-HSD test.

Figure 9. Spontaneous and METH-induced locomotor activity.

Time course of mice bilaterally injected with PBS (A) or IT (C) solution. After having been monitored for 1.5 hr, the mice were administered METH (2.0 mg/kg, *s.c.*), and movement score for 10-min period was measured. Locomotor activity of mice bilaterally injected with PBS (B) or IT (D) solution. The total number of movement score in a 30-min test period was calculated to evaluate spontaneous locomotor activity and METH-induced locomotor activity. *$p < 0.05$ versus the wild type spontaneous activity, **$p < 0.05$ versus the wild type METH-induced activity, significant differences according to the Tukey-HSD test.

Figure 10. Expression of gene markers correlated with neuronal activity.

Expression of SP mRNA in the striatum, GAD67 mRNA in the GP, and CO in the STN. The mRNA levels and CO activity were analyzed quantitatively with sections (10 μm thick for in

situ hybridization and 30 μm thick for CO histochemistry) prepared from unilaterally injected mice. The value is expressed as the ratio of the intensity of signals on the IT-injected side relative to that on the PBS-injected side. Open column, wild type mice (n = 5-7); closed column, mutant mice (n = 5-7). *$p < 0.01$, significant difference from the wild type value (Student's *t* test). Representative autoradiographic and histochemical images of the IT-injected side are shown in the right panel. Scale bar, SP and GAD67; 500 μm, CO; 100 μm.

Figure 11. Induction of IEGs in response to DA stimulation.

(A) c-*fos* induction detected by immunohistochemistry with sections (30 μm thick) prepared from unilaterally injected mice after METH treatment (6.0 mg/kg, *i.p.*). The values are expressed as the ratio of number of immunopositive neurons. Open column, wild type mice (n = 5 or 6); closed column, mutant mice (n = 5 or 6). *$p < 0.01$, significant difference from the wild type value (Student's *t* test). Light microscopic images of the IT-injected side are indicated. Scale bar, 100 μm. (B) *zif*268 induction in the striatum detected by immunohistochemistry with sections (30 μm thick) prepared from unilaterally injected mice after METH treatment (6.0 mg/kg, *i.p.*). The values are expressed as the ratio of number of immunopositive neurons. Open column, wild type mice (n = 5); closed column, mutant mice (n = 5). *$p < 0.01$, significant difference from the wild type value (Student's *t* test). Light microscopic images of the IT-injected side are indicated. Scale bar, 100 μm.

Figure 12. D1 class receptor agonist-mediated behavioral response.

Locomotor response to a selective D1 class receptor agonist. Bilaterally IT-injected mice were treated with saline or SKF81297 at low dose (0.5 mg/kg, *s.c.*) or high dose (2.0 mg/kg, *s.c.*).

Locomotor activity in a 30-min test period (10 min to 40 min after treatment) was measured. Open column, wild type mice (n = 3-8); closed column, mutant mice (n = 3-8). *$p < 0.01$, significant difference from the saline-treated mice (Tukey-HSD test).

Figure 13. Chemical lesion of striatal cholinergic interneurons.

(A) Mice were unilaterally administered AF64A or saline into the striatum and brain sections were taken. The sections (30 μm thick) through the striatum were immunostained with anti-choline acetyltransferase antibody. Scale bar, 200 μm. Open column, wild type mice (n = 4); closed column, mutant mice (n = 4). *$p < 0.01$, significant difference from the wild type value (Student's *t* test). (B) Locomotor activity. Mice (n = 6) were bilaterally treated with AF64A or saline, and used for measurement of spontaneous locomotor activity during the pretreatment and METH (2 mg/kg, *s.c.*)-induced locomotor activity. (C) c-*fos* induction. Unilaterally injected mice were administered METH (6 mg/kg, *i.p.*) and used for brain sectioning. The sections (30 μm thick) through the striatum were stained with anti-c-*fos* antibody. Scale bar, 100 μm. Open column, wild type mice (n = 4); closed column, mutant mice (n = 4).

Figure 14. Proposed models for the basal ganglia circuitry.

The excitatory and inhibitory pathways are illustrated by lines terminating with triangles and bars, respectively. EPN, entopeduncular nucleus; ST, striatum. (A) Basal state of the circuitry under the D2R-expressing neurons ablated condition. Open arrows indicate the upregulation or downregulation of neuronal activity under the neurons ablated condition relative to that under the normal condition. (B and C) DA-induced state of the circuitry under the normal (B) and the neurons ablated (C) conditions. Closed arrows indicate the regulation of neuronal

activity after DA stimulation, and the number of the arrows represents the relative strength of the activity between the two conditions. Grey arrow shows a possible facilitation of the striatonigral activity through the striatopallidal medium spiny neurons. See the text for detailed explanation.

Figure 1.

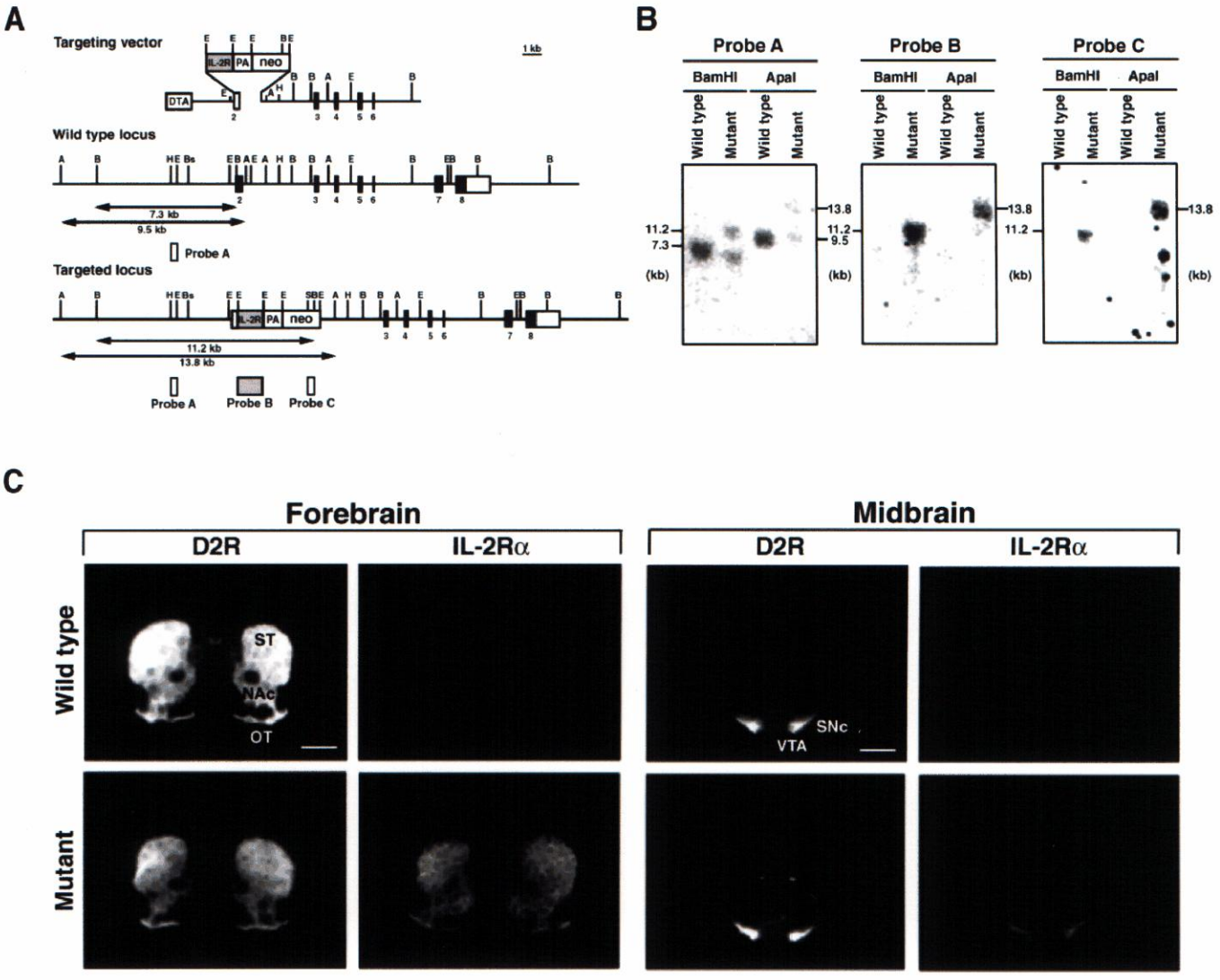
A
Targeting vector
1 kb
IL-2R
PA
neo
DTA
Wild type locus
7.3 kb
9.5 kb
Probe A
Targeted locus
11.2 kb
13.8 kb
Probe A
Probe B
Probe C
B
Probe A
Probe B
Probe C
BamHI
ApaI
Wild type
Mutant
11.2
7.3
13.8
9.5
(kb)
C
Forebrain
Midbrain
D2R
IL-2Rα
Wild type
Mutant
ST
NAc
OT
SNc
VTA

Figure 2.

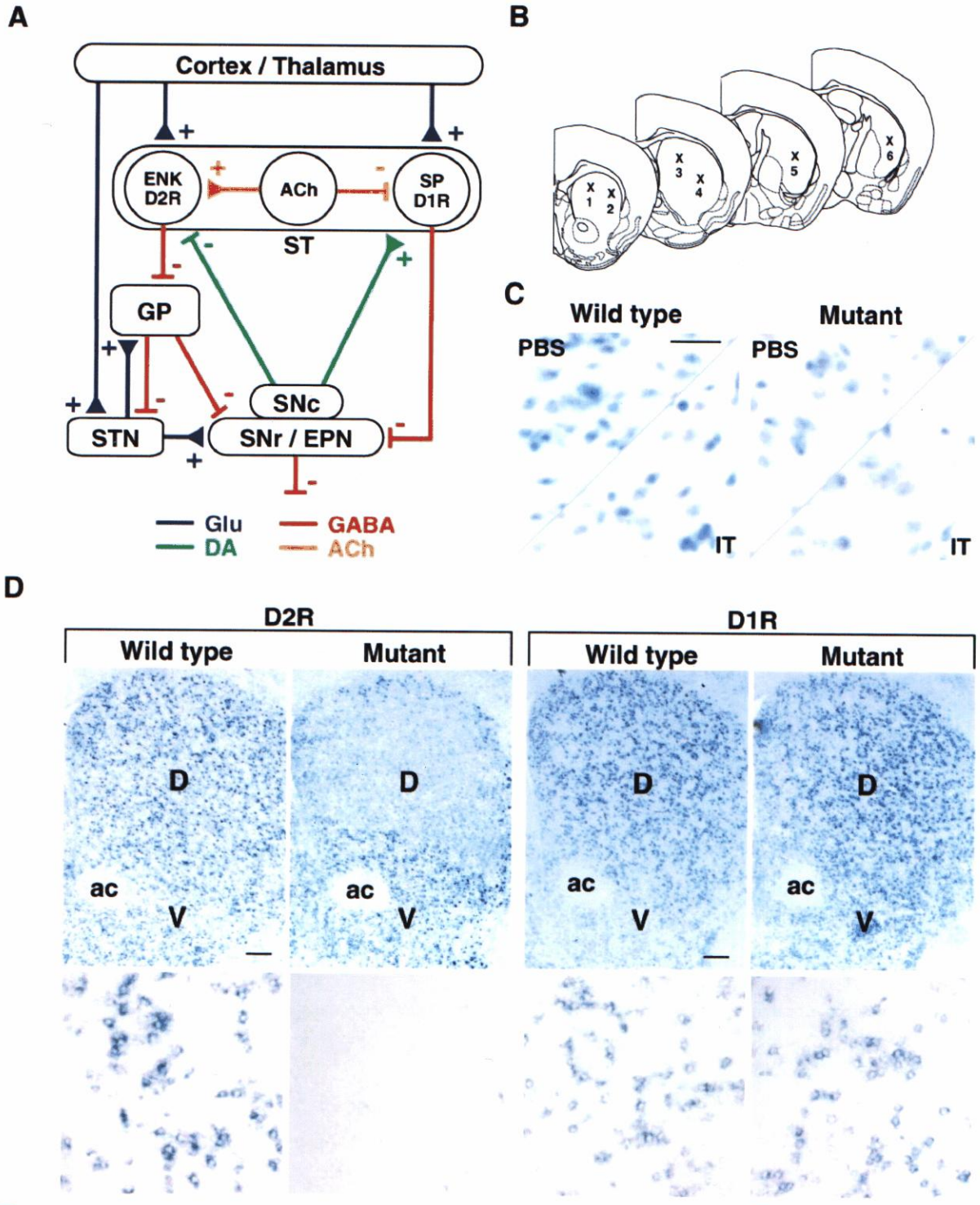
A
Cortex / Thalamus
ENK D2R
ACh
SP D1R
ST
GP
SNc
STN
SNr / EPN
Glu
DA
GABA
ACh
B
C
Wild type
Mutant
PBS
PBS
IT
IT
D
D2R
D1R
Wild type
Mutant
Wild type
Mutant
D
ac
V
E
D2R
D1R
Neuronal number
400
300
200
100
0
PBS
IT
F
Wild type
Mutant

Figure 3.

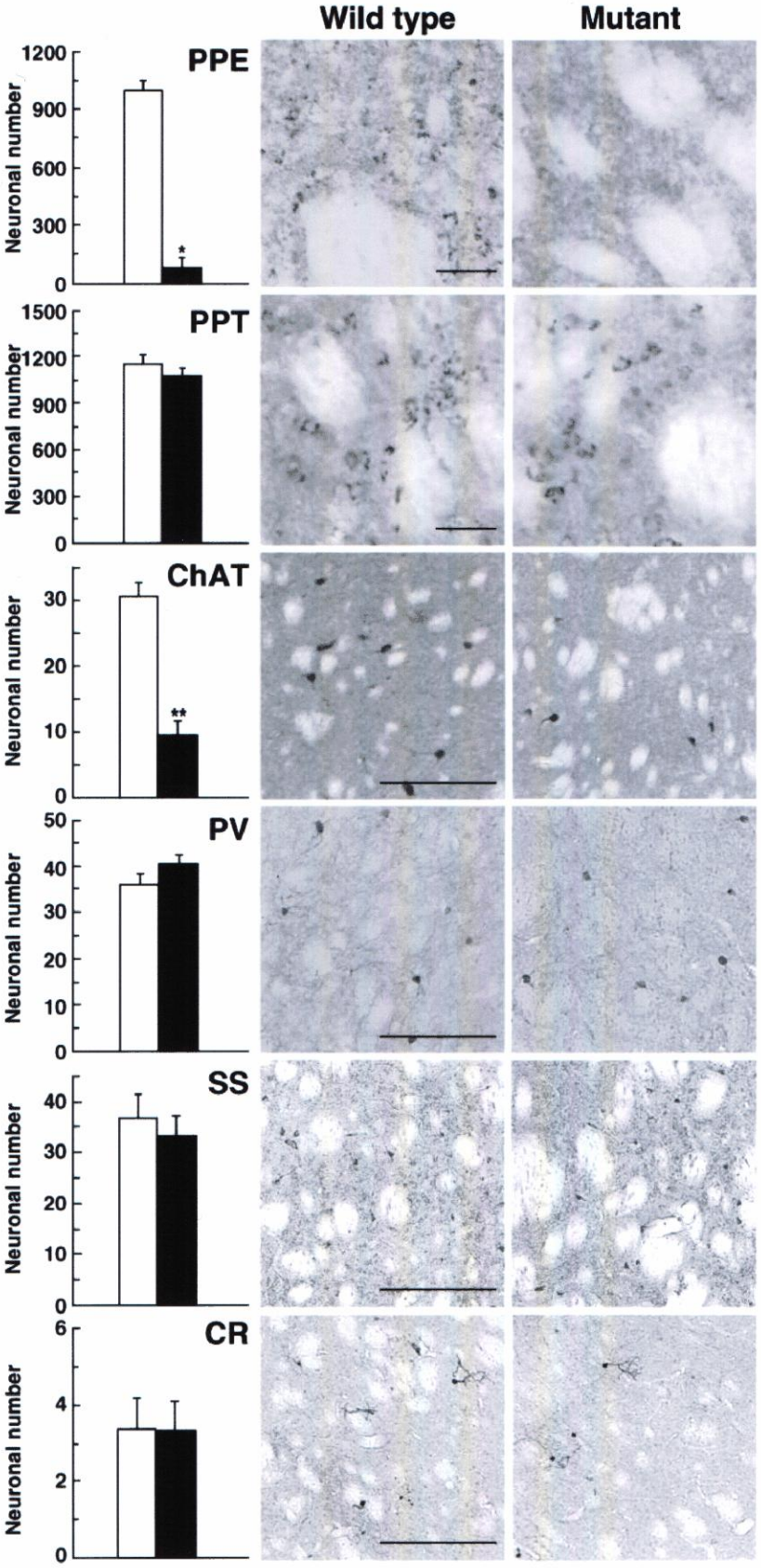
Wild type
Mutant
PPE
PPT
ChAT
PV
SS
CR
Neuronal number
1200
900
600
300
0
1500
30
20
10
50
40
6
4
2
*
**

Figure 4.

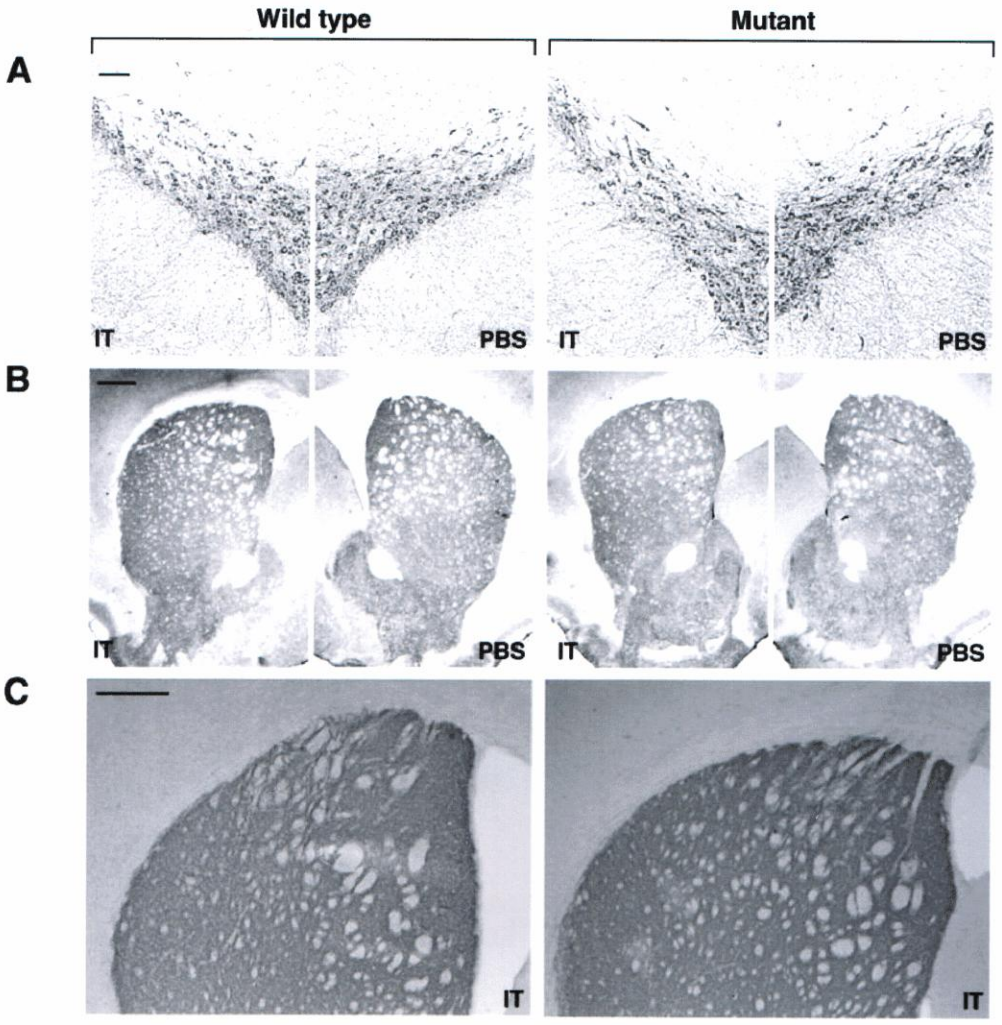

Figure. 5

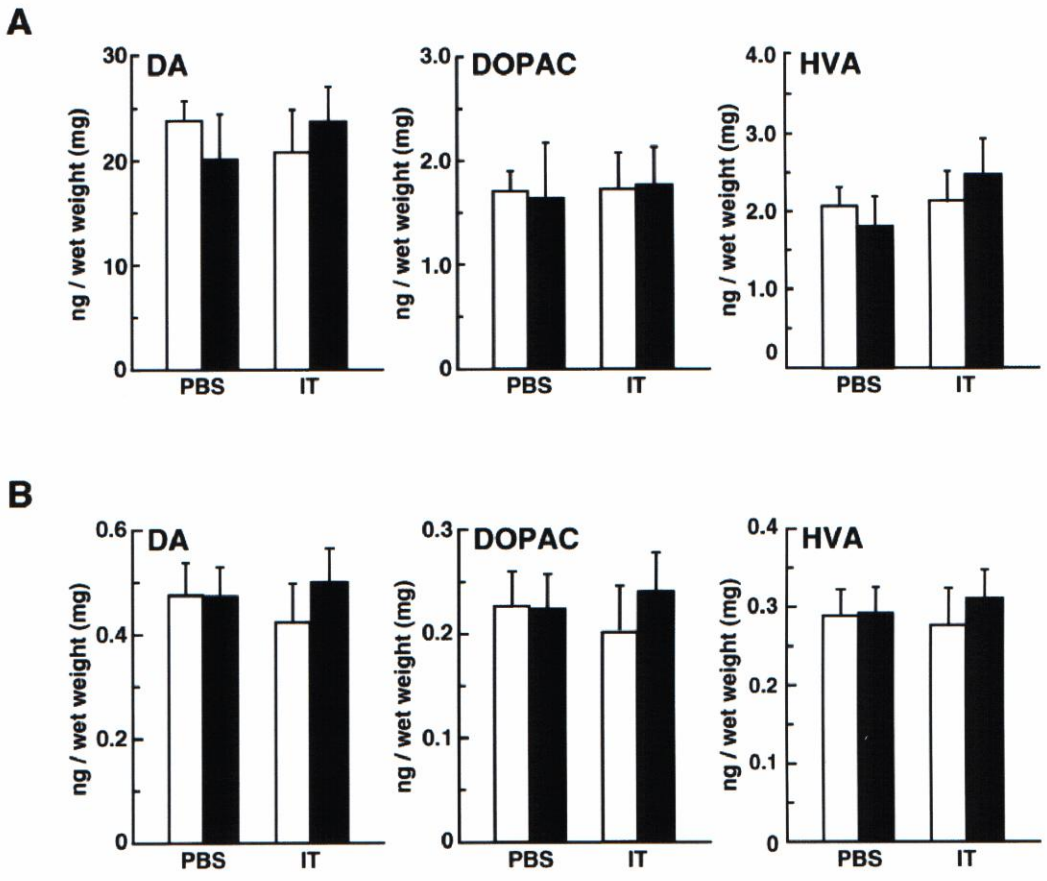
A
DA
DOPAC
HVA
ng / wet weight (mg)
30
20
10
0
3.0
2.0
1.0
4.0
PBS
IT
B
0.6
0.4
0.2
0.3
0.1

Figure 6.

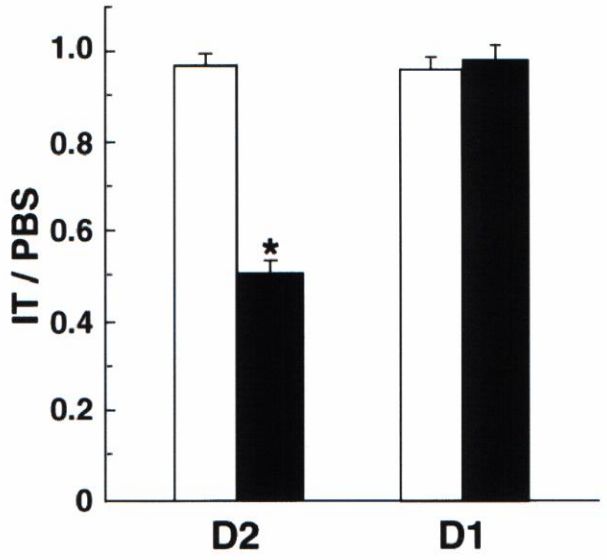

Figure 7.

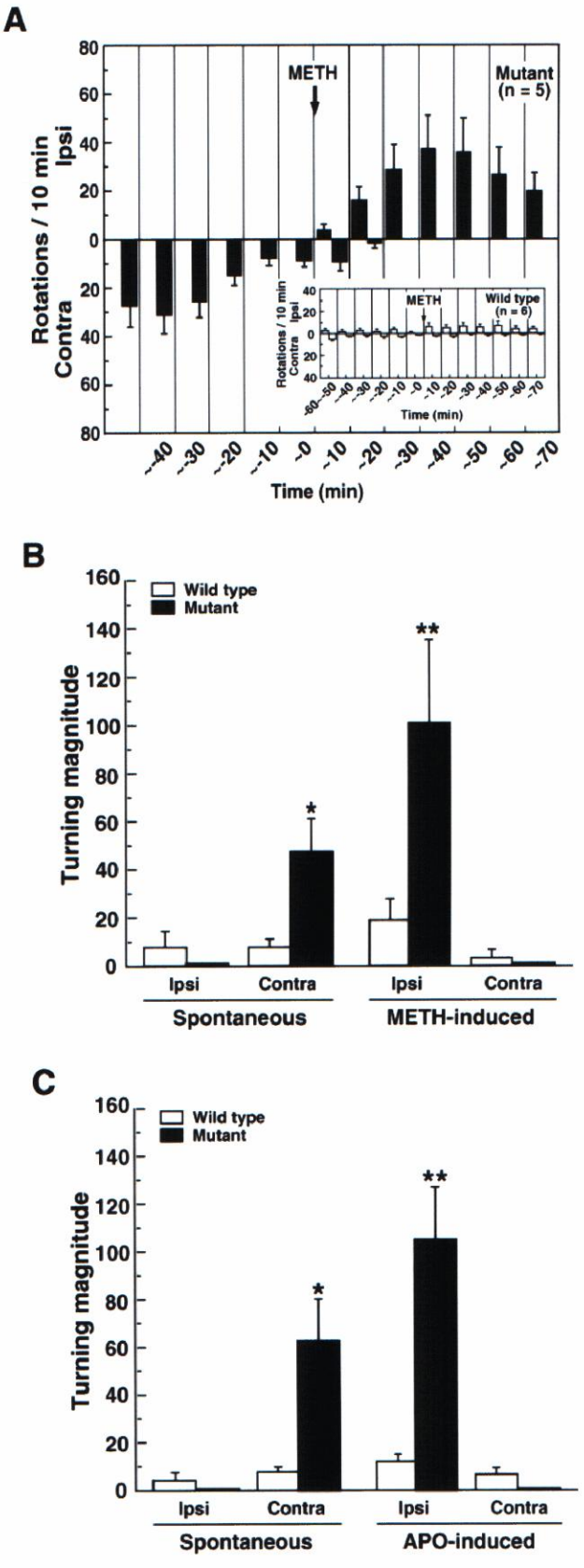
A
METH
Mutant
(n = 5)
Rotations / 10 min
Ipsi
Contra
Time (min)
Wild type
(n = 6)
B
Wild type
Mutant
Turning magnitude
Ipsi
Contra
Spontaneous
METH-induced
C
Wild type
Mutant
Turning magnitude
Ipsi
Contra
Spontaneous
APO-induced

Figure 8.

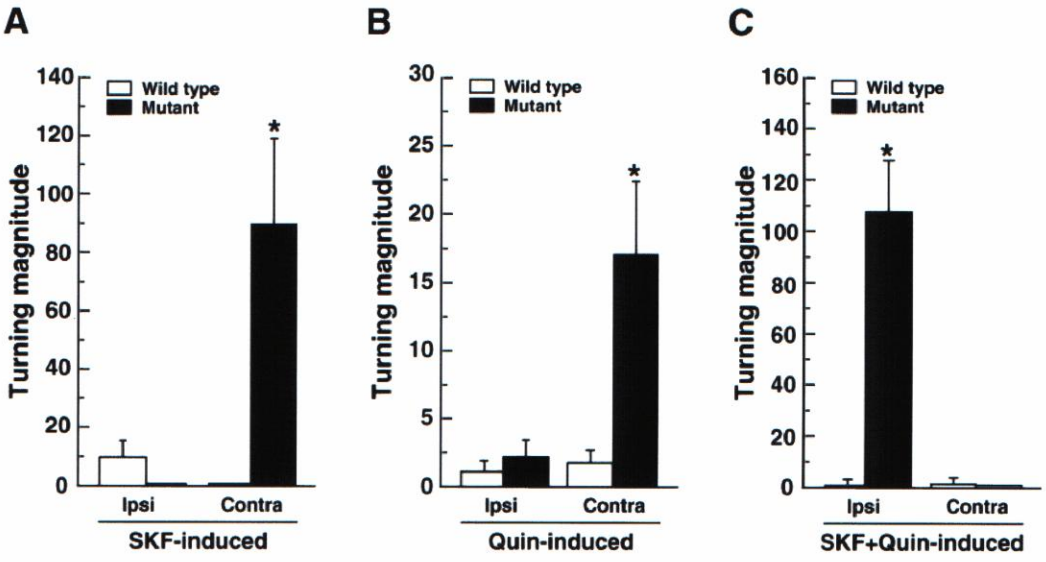
A
B
C
Wild type
Mutant
Turning magnitude
140
120
100
80
60
40
20
0
30
25
20
15
10
5
160
Ipsi
Contra
SKF-induced
Quin-induced
SKF+Quin-induced
*

Figure. 9

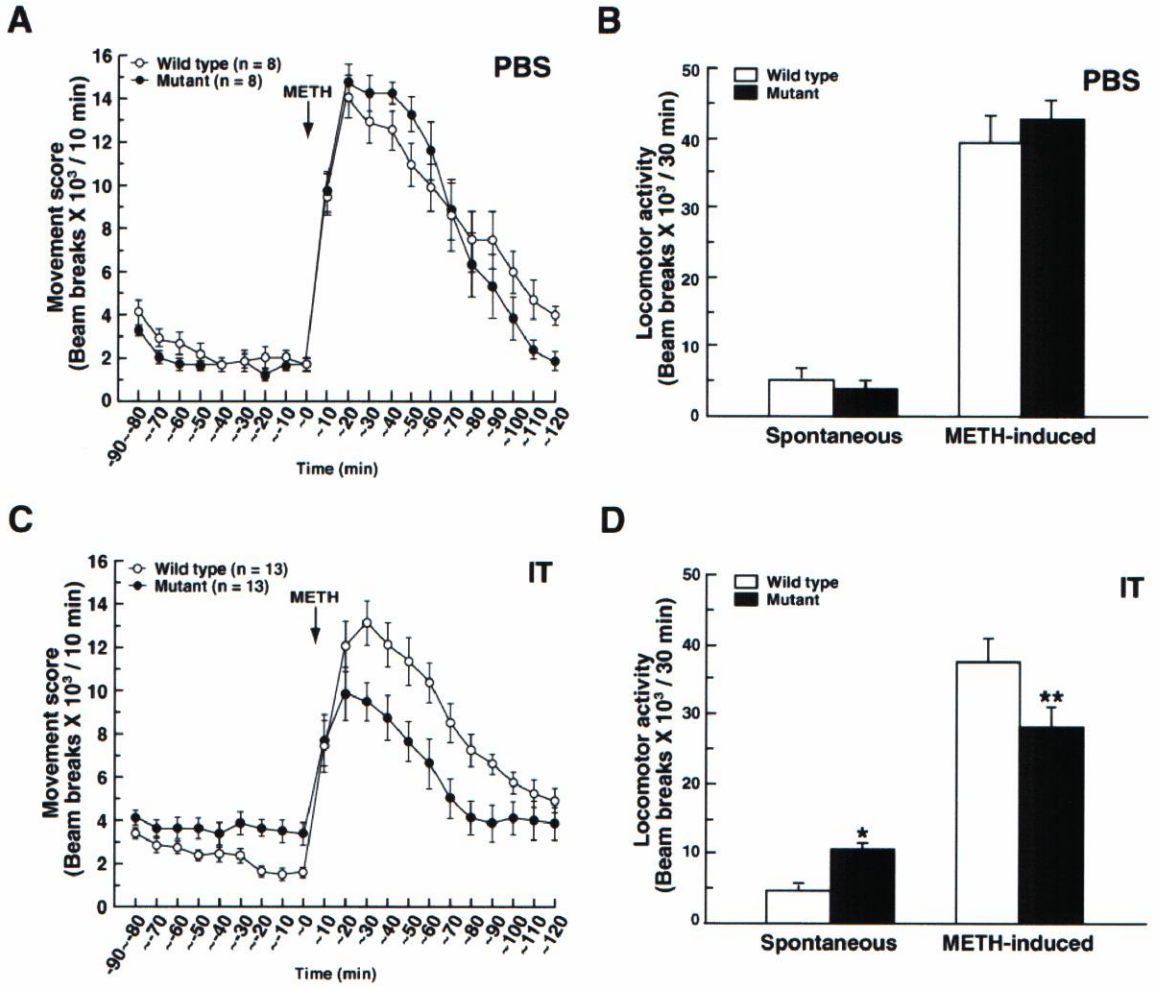
A
Wild type (n = 8)
Mutant (n = 8)
METH
PBS
Movement score
(Beam breaks X 10³ / 10 min)
Time (min)
B
Wild type
Mutant
PBS
Locomotor activity
(Beam breaks X 10³ / 30 min)
Spontaneous
METH-induced
C
Wild type (n = 13)
Mutant (n = 13)
METH
IT
Movement score
(Beam breaks X 10³ / 10 min)
Time (min)
D
Wild type
Mutant
IT
Locomotor activity
(Beam breaks X 10³ / 30 min)
*
**
Spontaneous
METH-induced

Figure 10.

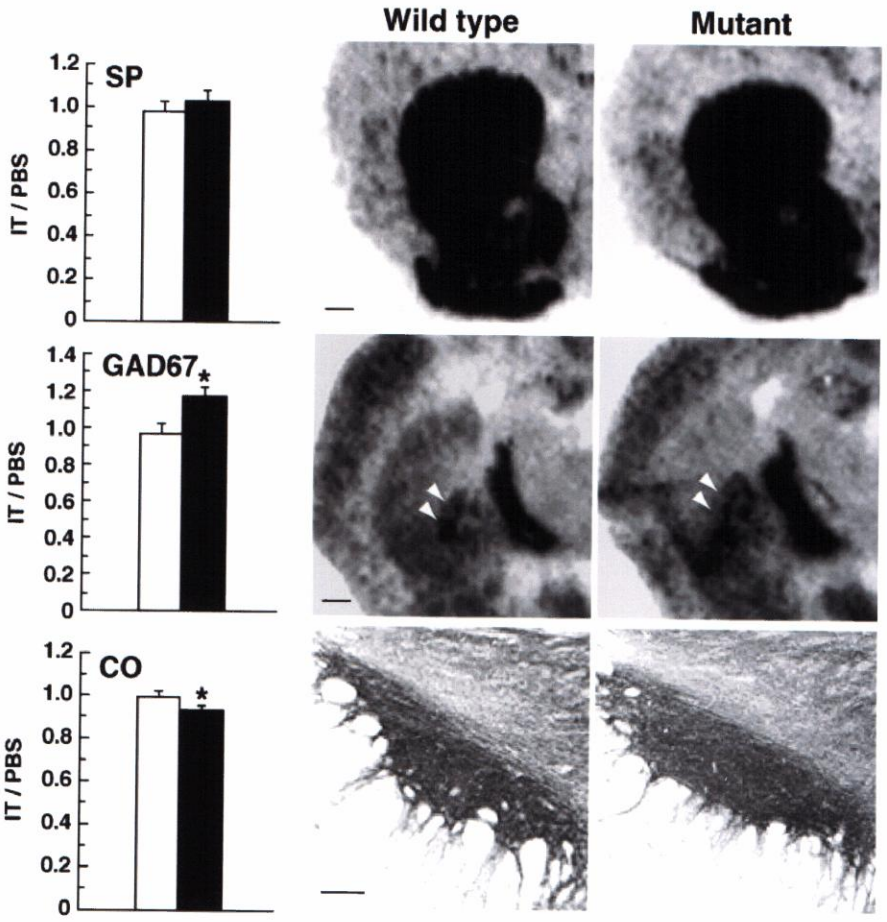

Figure 11.

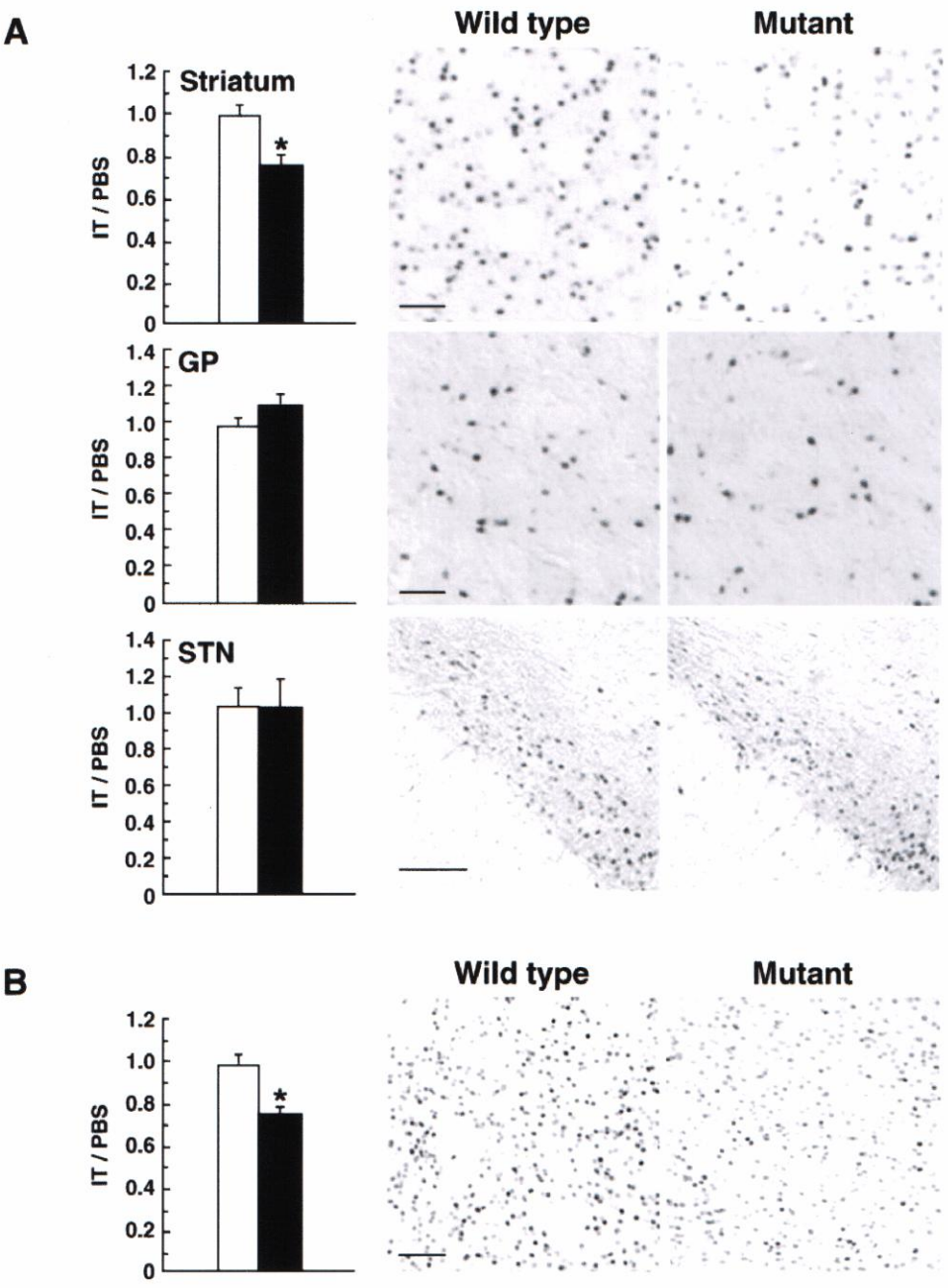
A
Wild type
Mutant
Striatum
GP
STN
IT / PBS
1.2
1.0
0.8
0.6
0.4
0.2
0
1.4
*
B
Wild type
Mutant
IT / PBS
1.2
1.0
0.8
0.6
0.4
0.2
0
*

Figure 12.

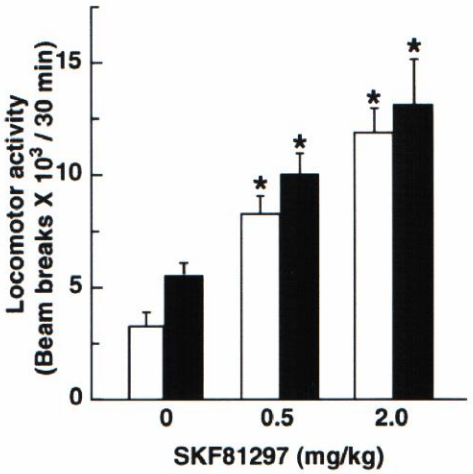
Locomotor activity
(Beam breaks X 10^3 / 30 min)
15
10
5
0
*
*
*
*
0
0.5
2.0
SKF81297 (mg/kg)

Figure 13.

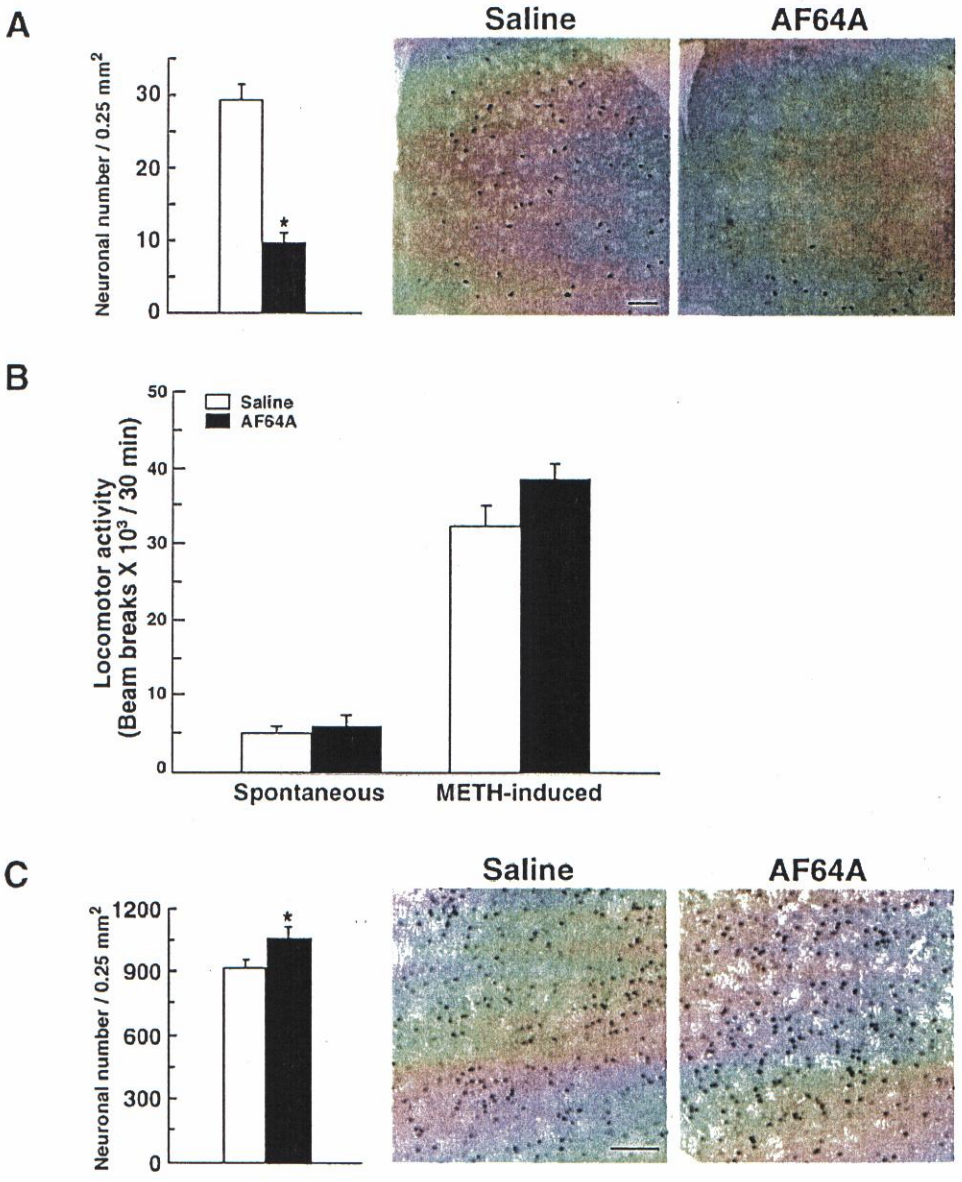
A
Saline
AF64A
Neuronal number / 0.25 mm2
30
20
10
0
*
B
Saline
AF64A
Locomotor activity
(Beam breaks X 10³ / 30 min)
50
40
30
20
10
0
Spontaneous
METH-induced
C
Saline
AF64A
Neuronal number / 0.25 mm2
1200
900
600
300
0
*

Figure 14.

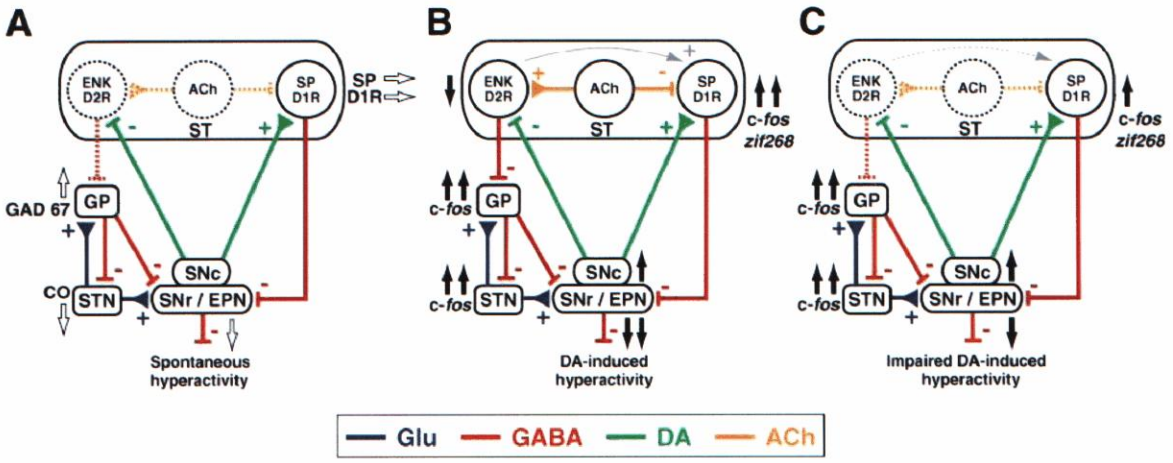
A
B
C
ENK D2R
ACh
SP D1R
SP D1R
ST
GAD 67
GP
SNc
CO
STN
SNr / EPN
Spontaneous hyperactivity
c-fos
zif268
DA-induced hyperactivity
Impaired DA-induced hyperactivity
Glu
GABA
DA
ACh